

## VOLTAGE-DEPENDENT CONDUCTANCES OF SOLITARY GANGLION CELLS DISSOCIATED FROM THE RAT RETINA

BY STUART A. LIPTON AND DAVID L. TAUCK

*From the Department of Neurology, Program in Neuroscience,  
Harvard Medical School and The Children's Hospital, Boston MA 02115, U.S.A.*

(Received 22 July 1986)

### SUMMARY

1. Ganglion cells were dissociated from the enzyme-treated rat retina, identified with specific fluorescent labels, and maintained *in vitro*. Electrophysiological properties of solitary retinal ganglion cells were investigated with both conventional intracellular and patch-clamp recordings. Although comparable results were obtained for most measurements some important differences were noted.

2. The input resistance of solitary retinal ganglion cells was considerably higher when measured with 'giga-seal' suction pipettes than with conventional intracellular electrodes. Under current-clamp conditions with both intracellular and patch pipettes, these central mammalian neurones maintained resting potentials of about  $-60$  mV and displayed action potentials followed by an after-hyperpolarization in response to small depolarizations. The membrane currents during this activity, analysed under voltage clamp with patch pipettes, consisted of five components:  $\text{Na}^+$  current ( $I_{\text{Na}}$ ),  $\text{Ca}^{2+}$  current ( $I_{\text{Ca}}$ ), and currents with properties similar to the delayed outward, the transient (A-type), and the  $\text{Ca}^{2+}$ -activated  $\text{K}^+$  currents ( $I_{\text{K}}$ ,  $I_{\text{A}}$  and  $I_{\text{K(Ca)}}$ , respectively).

3. Ionic substitution, pharmacological agents, and voltage-clamp experiments revealed that the regenerative currents were carried by both  $\text{Na}^+$  and  $\text{Ca}^{2+}$ .  $100$  nM– $1$   $\mu\text{M}$ -tetrodotoxin (TTX) reversibly blocked the fast spikes carried by the presumptive  $I_{\text{Na}}$ , which under voltage-clamp analysis had classical Hodgkin–Huxley-type activation and inactivation.

4. Single-channel recordings of the  $\text{Na}^+$  current ( $i_{\text{Na}}$ ) permitted comparison of these 'microscopic' events with the 'macroscopic' whole-cell current ( $I_{\text{Na}}$ ). The inactivation time constant ( $\tau_{\text{h}}$ ) fitted to the averaged single-channel recordings of  $i_{\text{Na}}$  in outside-out patches was slower than the  $\tau_{\text{h}}$  obtained during whole-cell recordings of  $I_{\text{Na}}$ .

5. In the presence of  $1$ – $40$   $\mu\text{M}$ -TTX and  $20$  mM-TEA, slow action potentials appeared in intracellular recordings and were probably mediated by  $\text{Ca}^{2+}$ . The potentials were abrogated by  $3$  mM- $\text{Co}^{2+}$  or  $200$   $\mu\text{M}$ - $\text{Cd}^{2+}$ ; conversely, increasing the extracellular  $\text{Ca}^{2+}$  concentration from  $2.5$  to  $10$ – $25$  mM or substitution of  $1$  mM- $\text{Ba}^{2+}$  for  $2.5$  mM- $\text{Ca}^{2+}$  enhanced their amplitude.  $I_{\text{Ca}}$  was measured directly in whole-cell recordings with patch pipettes after blocking  $I_{\text{Na}}$  with extracellular  $1$   $\mu\text{M}$ -TTX and  $\text{K}^+$  currents with intracellular  $120$ -mM  $\text{Cs}^+$  and  $20$  mM-TEA.

6. During whole-cell recordings with patch electrodes, extracellular 20 mM-TEA suppressed  $I_K$  and, to a lesser extent,  $I_A$ . Extracellular 5 mM-4-AP or a pre-pulse of the membrane potential to  $-40$  mV prior to stronger depolarization completely blocked  $I_A$ .

7. Following action potentials recorded with conventional intracellular microelectrodes, there was an after-hyperpolarization. The after-hyperpolarization was blocked by 3 mM- $\text{Co}^{2+}$ , 200  $\mu\text{M}$ - $\text{Cd}^{2+}$ , or 1 mM- $\text{Ba}^{2+}$ , suggesting that the current flowing during the after-hyperpolarization was at least in part  $\text{Ca}^{2+}$  sensitive and carried by  $\text{K}^+$ . During whole-cell recordings, a  $\text{Ca}^{2+}$ -activated outward current was also blocked by 3 mM- $\text{Co}^{2+}$  or 1 mM- $\text{Ba}^{2+}$  and represented  $I_{\text{K}(\text{Ca})}$ .

8. Single-channel recordings confirmed the existence of  $\text{Ca}^{2+}$ -activated  $\text{K}^+$  channels with a unitary conductance of  $\sim 115$  pS at  $34^\circ\text{C}$  in physiological solutions. Raising internal  $\text{Ca}^{2+}$  from  $10^{-8}$  M to 0.2–18  $\mu\text{M}$  or depolarizing the membrane beyond about  $-10$  mV activated these channels.

9. Provisional results from single-channel recordings indicated that at least two other channels with smaller unitary conductances but similar reversal potentials to  $I_{\text{K}(\text{Ca})}$  appear in these mammalian central neurones. The properties of one of these channels resembles those of  $I_K$ ; the other may possibly represent the channels carrying  $I_A$ .

10. Two subclasses of retinal ganglion cells could be distinguished in these cultures using antibodies against a specific neurofilament subunit. The two subclasses of ganglion cells displayed similar conductances in culture suggesting that disparate types of ganglion cells have these electrophysiological properties in common. These results suggest a varied repertoire of ion conductances in mammalian retinal ganglion cells.

#### INTRODUCTION

Retinal ganglion cells fire action potentials in response to specific variations in the pattern of illumination (Kuffler, 1953; Granit, 1955; Wiesel, 1959; Kaneko & Hashimoto, 1968). The precise role of ganglion cells in the visual perception of mammals is still unknown, but the centre-surround and 'on-off' organization of the receptive field reflects spatial and temporal processing of light stimuli (Kuffler, 1953; Barlow, Hill & Levick, 1964; Dowling & Boycott, 1966; Enroth-Cugell & Robson, 1966; Wässle & Boycott, 1974; Kolb, Nelson & Mariani, 1981; Wässle, Boycott & Illing, 1981). Recently, in ganglion cells in the intact retina of cat (Kirby & Schweitzer-Tong, 1981; Saito, 1981, 1983; Ikeda & Sheardown, 1982; Bolz, Frumkes, Voigt & Wässle, 1985*a*; Bolz, Thier, Voigt & Wässle, 1985*b*) and rabbit (Masland & Ames, 1976; Ariel & Daw, 1982*a, b*; Jensen & Daw, 1984), effects of  $\gamma$ -aminobutyric acid (GABA), glycine, dopamine and acetylcholine on receptive field properties have been observed. The drug responses, however, varied with different types of ganglion cells, and it was not clear what ionic conductance was affected by each agent (Daw, Ariel & Caldwell, 1982). In order to understand the receptive field properties at a cellular level, it will be important to discover how various ionic conductances in the membrane contribute to these properties. The first step in this approach is to characterize the membrane conductances of the ganglion cells.

Electrophysiological recordings in the intact retina allow the natural stimulus, light, to be used to monitor the health of the preparation and the physiological response of the ganglion cells to various drugs. Disadvantages of the intact retinal preparation, however, are also evident: presumptive ganglion cells, that are labelled with fluorescent dyes or horseradish peroxidase (HRP) during the recording session, cannot be identified in histological sections until after the experiment. Most importantly, because many cells are present, it is generally impossible to be certain if an exogenously applied drug is acting on the neurone under study or by modulating the level of an endogenous compound that is released from a second-order cell. In addition, in the intact retina, the various ionic currents of the ganglion cells often cannot be separated; because of long processes or the presence of electrical coupling between cells, there is a poor space clamp which precludes an adequate voltage clamp that is necessary to examine individual currents. Finally, it is difficult to impale mammalian ganglion cells in a stable manner with micro-electrodes *in situ* (Wiesel, 1959; Nelson, Famiglietti & Kolb, 1978; Dacheux & Miller, 1981; Zrenner, Nelson & Mariani, 1983; Bloomfield & Dowling, 1985), possibly because of their relatively small size and the fact that they comprise only about 1% of all retinal cells.

One way to examine membrane properties without the complexities of the intact retina is to study solitary ganglion cells from enzymatically dissociated retinas. Solitary cells have no synaptic connexions to other neurones. Previous workers have demonstrated the feasibility of isolating other types of cells from the vertebrate retina (Bader, MacLeish & Schwartz, 1979; Sarthy & Lam, 1979; Tachibana, 1981; Lasater & Dowling, 1982; Lipton, 1983, 1985*a*; Dowling, Pak & Lasater, 1985; Kaneko & Tachibana, 1985), and recently techniques have been developed in this laboratory to obtain cultures of solitary mammalian ganglion cells that can be identified with specific fluorescent probes (Leifer, Lipton, Barnstable & Masland, 1984). By plating the cells on plain glass, they become spatially compact (lack long processes), permitting separation of whole-cell currents using a voltage-clamp technique; since the cells have been enzymatically cleansed, patch electrodes can be used (Hamill, Marty, Neher, Sakmann & Sigworth, 1981).

The solitary ganglion cells studied in the present investigation were obtained from rat retinas and cultured for up to 1 week. During this time the ionic conductances of the membrane were studied with both intracellular and patch electrodes. Comparing results obtained with the two techniques permitted the analysis of discrepancies and the avoidance of possible artifacts associated with each method. The action potentials of retinal ganglion cells have discrete  $\text{Na}^+$  and  $\text{Ca}^{2+}$  components (representing the currents  $I_{\text{Na}}$  and  $I_{\text{Ca}}$ , respectively). Delayed outward ( $I_{\text{K}}$ ) and transient A-type ( $I_{\text{A}}$ ) currents probably contribute to repolarization and possibly the interspike interval. Repolarization is followed by a  $\text{Ca}^{2+}$ -sensitive after-hyperpolarization that is probably mediated by a  $\text{K}^+$  current ( $I_{\text{K(Ca)}}$ ).

#### METHODS

##### *Identification, dissociation and culture of cells*

Retinal ganglion cells were labelled *in situ* by retrograde transport of the fluorescent dyes granular blue, Evans Blue or Lucifer Yellow VS coupled to wheat-germ agglutinin (Leifer *et al.* 1984). These dyes were injected using a fine needle into the superior colliculus and lateral geniculate

nucleus of pigmented (Long Evans) rats under cryoanaesthesia on postnatal day 4. At this age all of the central connexions of the adult have already been formed and in this sense the cells are fully differentiated (for references, see Leifer *et al.* 1984). The use of a variety of fluorescent dyes (both nuclear and cytoplasmic) ensured that no one marker adversely affected the cells. 2 days after the injection the animals were sacrificed by cervical dislocation. The retinas were enucleated from the eyes and dissociated by gentle trituration following digestion with papain, as previously described (Leifer *et al.* 1984). The isolated ganglion cells could be unequivocally identified by the fluorescence of transported dye as well as by a second probe, a monoclonal antibody against Thy-1, which is specific for ganglion cells *in vitro* (for photographic illustrations see Figs. 1 and 2 in Leifer *et al.* 1984). In either case, during the identification process the light necessary to excite the fluorescent chromophore illuminated the cells for only a few seconds in order to minimize damage from this irradiation. The retinal cells were cultured in Eagle's minimal essential media (Gibco) with methylcellulose (0.7% w/v), glutamine (2 mM), gentamicin (1  $\mu\text{g/ml}$ ), glucose (16 mM) and rat serum (5% v/v). Ganglion cells were generally plated on plain glass for electrophysiological recordings to encourage a spatially compact configuration. Additional recordings were performed on cells attached to the dish by a monoclonal antibody to Thy-1 which enhances process regeneration (Leifer *et al.* 1984). Retinal ganglion cells that had regenerated neural processes exhibited the same voltage-dependent conductances as those without processes. Solitary ganglion cells in culture survived for up to a week while ganglion cells in contact with small clusters of other retinal cells remained viable for up to 2½ weeks (Leifer *et al.* 1984).

In addition, a subpopulation of retinal ganglion cells could be identified based upon their large size and staining characteristics with antibodies against the 145000 molecular weight subunit of neurofilaments (Dräger & Hofbauer, 1984). The use of these antibodies allowed us to distinguish between at least two subclasses of these mammalian central neurones.

#### *Electrophysiological recordings*

Conventional intracellular recordings from eighty-one retinal ganglion cells of 5–20  $\mu\text{m}$  in diameter were made at 30–36 °C with fine pipettes. When filled with 4 M-potassium acetate, the micro-electrode resistances were 150–200 M $\Omega$ . Current was injected into cells via a recording-stimulating chopping circuit that has been described elsewhere (Bader *et al.* 1979; Lipton, 1983). In addition to recordings of transmembrane potential, in order to analyse the membrane properties of the cells it was necessary to separate the various ionic currents using a voltage-clamp procedure. Although relatively slow currents (time constant greater than 100 ms) could be recorded using a standard micropipette for single-electrode voltage clamp (Bader *et al.* 1979; Lipton, 1983), currents with faster kinetics such as Na<sup>+</sup> and Ca<sup>2+</sup> currents, could not be accurately measured with this technique.

To circumvent this problem, patch-clamp recordings were made from 304 solitary ganglion cells following the methods of Hamill *et al.* (1981) using an EPC-7 amplifier (List Electronic, Darmstadt, F.R.G.). Patch electrodes had resistances of 3–5 M $\Omega$  when filled with Na<sup>+</sup> or K<sup>+</sup> saline. Patch electrodes were used to record whole-cell currents under voltage clamp as well as single-channel currents from patches of membrane excised from the cell. The indifferent electrode was a Ag–AgCl wire connected to the culture dish via an agarose bridge. Holding and command potentials ( $V_H$  and  $V_C$ , respectively) were generated by a digital-to-analog converter (Cheshire Data, Hamden, CT, U.S.A.) interfaced with a PDP 11/23 or 11/73 computer (Digital Equipment Corp., Maynard, MA, U.S.A.). Data collection was also controlled by the computer; data were sampled and digitized with a 12-bit, 125 kHz analog-to-digital converter (Data Translation, Marlboro, MA, U.S.A., Model DT2782 DMA) and viewed on a Hewlett-Packard digital display (Model 1345A). The sampling rate was set at 10  $\mu\text{s}$  to 50 ms depending on the level of analysis. Using the amplifier test circuit, the digitized data were accurate to within 1%. The signals were low-pass filtered at a setting appropriate to the sampling frequency (Ithaco, Ithaca, NY, U.S.A., Model 4302 with a Bessel frequency cut-off characteristic of 48 dB/octave). Leakage currents and liquid junction potentials were corrected as described in Fenwick, Marty & Neher (1982a). Using the EPC-7 circuit, analog compensation of the series resistance was applied. This ensured a relatively small error due to the voltage drop across the series resistance (less than or equal to that calculated by Marty & Neher, 1985). Data were stored on a 30 megabyte Winchester disk (Data Systems Design, San Jose, CA, U.S.A., Model 880). For long-term storage data files were transferred to a streaming tape (Alloy Computer Products, Marlborough, MA, U.S.A., Model LSI-50).

*Superfusion system and solutions*

The recording dish contained a stainless-steel insert which limited the fluid volume in the dish to approximately 100  $\mu$ l. The solution was constantly changed by continuous superfusion at 0.8 ml/min. Various ionic changes and drug addition were made in the superfusate resulting in a maximal concentration change within approximately 1 min ( $\pm 15\%$  from dye studies). In some cases drugs were added more acutely by microperfusion via a pneumatic pipette (tip diameter 10–30  $\mu$ m). The bath solution generally contained a Na<sup>+</sup> saline based upon Hanks' balanced salts (mM): NaCl, 137; NaHCO<sub>3</sub>, 1; Na<sub>2</sub>HPO<sub>4</sub>, 0.34; KCl, 5.4; KH<sub>2</sub>PO<sub>4</sub>, 0.44; CaCl<sub>2</sub>, 2.5; MgSO<sub>4</sub>, 0.5; MgCl<sub>2</sub>, 0.5; HEPES–NaOH, 5; glucose, 22.2; pH 7.2 with Phenol Red indicator (0.001%) in the solution. K<sup>+</sup> saline, to which the internal side of the membrane was exposed in inside-out patches and whole-cell experiments, typically contained 140 mM-KCl, 2 mM-MgCl<sub>2</sub>, a Ca–EGTA buffer, and 10 mM-HEPES–NaOH buffer at pH 7.2. The internal Ca<sup>2+</sup> concentration was calculated (Caldwell, 1970) to be  $2 \times 10^{-7}$  M with 1.5 mM-EGTA–1 mM-CaCl<sub>2</sub> and  $10^{-8}$  M with 11 mM-EGTA–1 mM-CaCl<sub>2</sub>. For studies on whole-cell currents carried by Na<sup>+</sup> and Ca<sup>2+</sup>, it was necessary to suppress outward currents, so pipettes were generally filled with a Cs<sup>+</sup>- and tetraethylammonium (TEA)-rich solution of the following composition (mM): CsCl, 120; TEACl, 20; EGTA–NaOH, 1.5 or 11; CaCl<sub>2</sub>, 1; MgCl<sub>2</sub>, 2; HEPES–NaOH, 10; pH 7.2. Deviations from these solutions are indicated in the Figure legends.

## RESULTS

*Comparison of recordings from labelled and unlabelled ganglion cells*

Electrical recordings were made from a total of 389 solitary mammalian retinal cells during the course of these experiments; 375 neurones were identified as ganglion cells by the presence of retrogradely transported fluorescent dye. Additionally, a patch pipette was used to record from a small number of unlabelled cells that were thought to be ganglion cells on the basis of morphology alone ( $n = 14$ ). Ten of these fourteen neurones proved to be ganglion cells after the recording session by immunofluorescence with Thy-1 antibody. Similar electrical properties were observed in the ganglion cells identified with Thy-1 antibody *after* the recording and in cells retrogradely labelled *prior* to recording. Thus, by this criterion the presence of fluorescent dyes did not appear to be harmful to the neurones under these conditions.

*Recordings from subclasses of ganglion cells*

Of all the ganglion cells identified with retrograde label in culture, only the cells with a somal diameter of at least 16  $\mu$ m stained with the neurofilament antibodies (U. C. Dräger & S. A. Lipton, in preparation). These large cells probably correspond to the  $\alpha$  or Y-like ganglion cells (see below). Electrical properties, however, did not vary with the size of the cell; cell types both larger and smaller than 16  $\mu$ m shared the currents described below.

*Passive electrical properties*

With intracellular pipettes the resting potential of retinal ganglion cells was measured at a mean of  $-60 \pm 7.9$  mV (mean  $\pm$  s.d.,  $n = 27$ ). The input resistance, determined from 5–25 mV hyperpolarizing pulses, was 250–300 M $\Omega$  for cells that were 10–20  $\mu$ m in diameter and lacked long processes. With patch electrodes filled with K<sup>+</sup> saline containing 0.2  $\mu$ M-free Ca<sup>2+</sup>, the resting potentials were comparable when measured in the current-clamp mode as soon as a whole-cell recording was

established. However, the input resistance was higher, generally 850 M $\Omega$  to 3 G $\Omega$ . This discrepancy will be discussed later.

### *Spontaneous regenerative activity*

With intracellular or patch electrodes, solitary ganglion cells only rarely displayed spontaneous action potentials whereas about 50% of the ganglion cells located in clusters of other retinal cells had spontaneous spikes (based upon recordings from

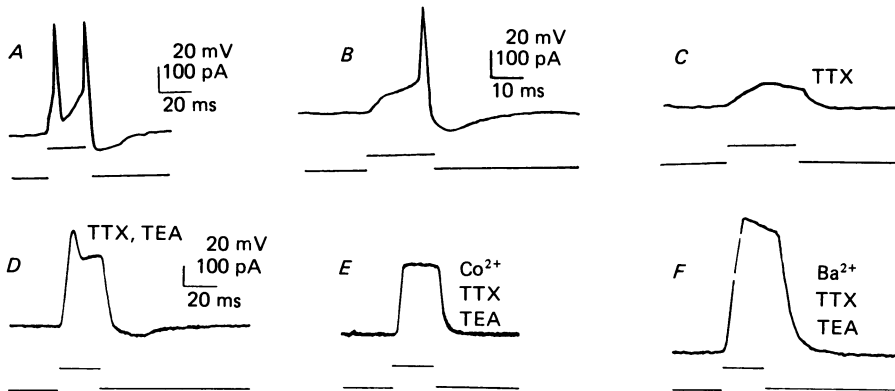


Fig. 1. Physiology of solitary retinal ganglion cells in culture. Records of the transmembrane potential obtained with intracellular pipettes. Records *A–C* are from the same cell and *D–F* from another cell. Temperature 35 °C. *A*, a depolarizing current stimulus of 100 pA (bottom trace) triggered two action potentials followed by an after-hyperpolarization. *B*, a single action potential was elicited by a 50 pA depolarizing stimulus. *C*, 1  $\mu$ M-TTX blocked the action potential. *D*, treatment with 40  $\mu$ M-TTX and 20 mM-TEA resulted in a slower all-or-none potential followed by a small after-hyperpolarization. *E*, in 3 mM- $\text{Co}^{2+}$  both the slow action potential and after-hyperpolarization were blocked. *F*, after washing out the  $\text{Co}^{2+}$ , 1 mM- $\text{Ba}^{2+}$  gave rise to a larger, more prolonged action potential that was not followed by an after-hyperpolarization. For those traces without scale bars, the calibration is the same as in the preceding panel.

ninety-four clustered ganglion cells). The spontaneous spikes were often accompanied by post-synaptic potentials and presumably reflect synaptic input in these cell clusters (Lipton, 1986). The remainder of the results are based upon recordings from solitary retinal ganglion cells.

### *Intracellular recordings with conventional micro-electrodes*

All of the ganglion cells studied produced multiple spikes in response to small depolarizing stimuli, as shown in Fig. 1 *A*, and at least one spike with anode break. These spikes were followed by a brief after-hyperpolarization.

It is clear from previous studies that in other types of neurones the current of the rising phase of the fast action potential is carried by  $\text{Na}^+$  and blocked by tetrodotoxin (TTX). Also, in many types of neurones, the after-hyperpolarization is mediated at least in part by a  $\text{K}^+$  conductance that is activated by  $\text{Ca}^{2+}$  entering during the action potential (Alger & Nicoll, 1980, but note that the delayed outward-rectifying

TABLE 1. Effect of increased external  $[Ca^{2+}]$  on the amplitude of the slow action potential

External $[Ca^{2+}]^*$ (mM)	Increase in amplitude (mV; mean $\pm$ s.d.)	Prediction from Nernst equation (mV at 35 °C)
10	12.7 $\pm$ 1.4	18.5
20	24.9 $\pm$ 5.5	27.7
25	28.3 $\pm$ 6.1	30.7

\* The control solution contained 2.5 mM- $Ca^{2+}$ .

conductance may also contribute to the after-hyperpolarization as well as to the repolarization phase of the action potential). In addition, an inward  $Ca^{2+}$  current can often be unmasked by diminishing the outward  $K^+$  currents with TEA (for a review, see Hagiwara & Byerly, 1981). These pharmacological agents were used to gather indirect evidence for the presence of these conductances in retinal ganglion cells.

*Effects of TTX on fast action potentials.* The addition of 0.1–40  $\mu$ M-TTX to the bath reversibly blocked the fast component of the action potential (Figs. 1B and C, and 2); in the presence of TTX, increasing the current stimulus fivefold still did not result in an action potential. These findings indicate that the spike is TTX sensitive and that the current of the rising phase is most likely carried by  $Na^+$ . Substitution of choline<sup>+</sup> or Tris<sup>+</sup> for 30–137 mM- $Na^+$  resulted in an irreversible decrement in the amplitude of the action potential ( $n = 12$ ). This 'rundown' may be technically unavoidable because these postnatal mammalian neurones appear to be very sensitive to changes in the extracellular ionic milieu.

*Slow action potentials and effects of divalent cations.* When 40  $\mu$ M-TTX and 20 mM-TEA were added together, the fast spike disappeared, but an increased depolarizing stimulus elicited a slower action potential followed by a small after-hyperpolarization (Fig. 1D). This potential had regenerative characteristics since it did not appear until threshold was reached, did not vary in size when elicited by suprathreshold stimuli, and could be triggered by anode break (not illustrated). The slow action potential was reversibly blocked by 3 mM- $Co^{2+}$  (Fig. 1E) or 200  $\mu$ M- $Cd^{2+}$  and increased by 1 mM- $Ba^{2+}$  (Fig. 1F). The after-hyperpolarization was abolished by all three of these cations (Fig. 1E for  $Co^{2+}$  and Fig. 1F for  $Ba^{2+}$ ;  $n = 9$ ). In many types of neurones  $Co^{2+}$  and  $Cd^{2+}$  block  $Ca^{2+}$  channels (Hagiwara, 1983).  $Ba^{2+}$  is known to substitute for  $Ca^{2+}$  and increase the amplitude of the slow action potential while diminishing a  $Ca^{2+}$ -activated  $K^+$  conductance (Hagiwara & Naka, 1964; Alger & Nicoll, 1980). Therefore, one interpretation of these findings is that the slow action potential is mediated by inward  $I_{Ca}$  and that the resulting increase in intracellular  $Ca^{2+}$  concentration triggers  $I_{K(Ca)}$  that is responsible at least in part for the after-hyperpolarization in these mammalian central neurones.

If the upstroke of the slow action potential were produced by an influx of  $Ca^{2+}$ , then the amplitude of the action potential should vary with the extracellular  $Ca^{2+}$  concentration. Table 1 summarizes the effects of bathing solitary retinal ganglion cells in different  $Ca^{2+}$  levels for 10 min. The mean increase in amplitude correlates well with that predicted from the Nernst equation, suggesting that under these conditions the cells function like a  $Ca^+$  electrode near the peak of the slow action potential. However, the empirical values were somewhat smaller than those predicted.

Taken together, the experiments with divalent cations strongly suggest that  $\text{Ca}^{2+}$  is the ion which carries the inward current during the upstroke of the slow action potential in solitary retinal ganglion cells.

*Whole-cell and single-channel inward currents recorded with patch electrodes*

*Effects of TTX on inward current.* In addition to the conventional intracellular recordings, more definitive evidence for the ionic basis of the regenerative activity,

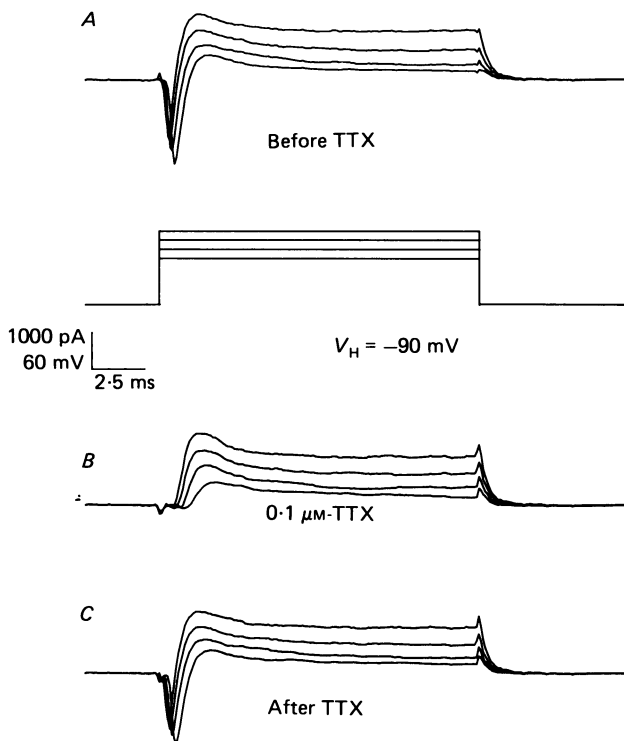


Fig. 2. Reversible block of inward current by TTX. Voltage steps (bottom set of traces in *A*) were applied to a retinal ganglion cell during whole-cell recording with a patch pipette. The cell was held at  $-90$  mV to remove inactivation of  $I_{\text{Na}}$ . The inward currents (shown as downward deflexions in *A*) were blocked by the addition of  $0.1 \mu\text{M}$ -TTX (in *B*) while outward current was little affected. *C*, by washing out TTX, the action was reversed. The bath contained  $\text{Na}^+$  saline and the pipette,  $\text{K}^+$  saline with  $2 \times 10^{-7}$  M- $\text{Ca}^{2+}$  (see Methods for composition). Because this cell had been recorded from for some time before these records were obtained,  $I_{\text{Ca}}$  had markedly declined. Temperature  $33^\circ\text{C}$ ; 5 kHz low-pass filter.

repolarization, and after-hyperpolarization was obtained from whole-cell and single-channel current recordings. Fig. 2 illustrates a composite of whole-cell current records with  $\text{K}^+$  saline in the pipette. A large component of the inward current was reversibly blocked by the addition of  $0.1 \mu\text{M}$ -TTX to the bath, presumably indicating an ionic selectivity for  $\text{Na}^+$ . The nature of the outward currents will be described after the inward ones. The terms inward and outward currents are used to describe the

predominant direction of current flow in the physiological range of membrane potentials.

$I_{Na}$  and  $I_{Ca}$ . One set of experiments was performed under conditions when  $I_{Na}$  and  $I_{Ca}$  were isolated. This was accomplished by suppressing the outward  $K^+$  currents

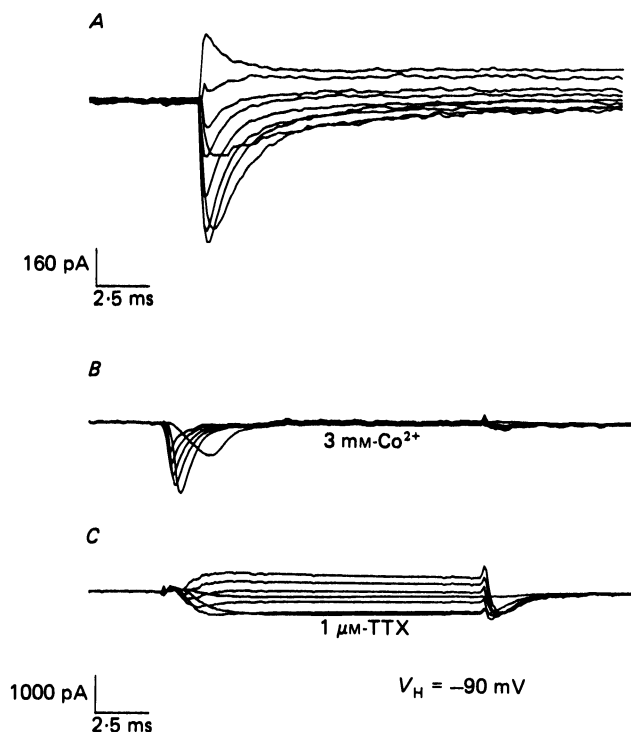


Fig. 3.  $I_{Na}$  and  $I_{Ca}$  in whole-cell recording using a patch pipette. The bath contained Na<sup>+</sup> saline and the pipette, the Cs<sup>+</sup>-TEA internal solution with  $2 \times 10^{-7}$  M-Ca<sup>2+</sup> (see Methods for composition). *A*, the superimposed current traces are for depolarizations starting from a holding potential ( $V_H$ ) of  $-70$  mV to command potentials ( $V_C$ ) of  $-30$ ,  $-20$ ,  $-10$ ,  $0$ ,  $10$ ,  $20$ ,  $30$ ,  $40$  and  $60$  mV. Each trace is a single sweep after subtraction of linear leak and capacitive currents. A period of  $100 \mu s$  has been removed at the time of the step depolarization. The input resistance determined from small hyperpolarizing pulses, after the cell had been dialysed with the Cs<sup>+</sup>-rich solution, was  $10 G\Omega$ . Analog compensation for the series resistance was employed using the circuit in the EPC-7 amplifier; the series resistance calculated from the  $G_{series}$  setting of the amplifier was  $11 M\Omega$ . Further analysis of the same cell is shown in Figs. 4*D* and 5. *B*, *C*, in another cell  $I_{Na}$  and  $I_{Ca}$  were isolated from one another. A series of voltage steps was applied during whole-cell recording from  $V_H = -90$  mV to various command potentials in  $15$  mV increments ( $V_C = -45$  to  $+30$  in *B* and  $-30$  to  $+60$  mV in *C*). In *B*,  $3$  mM-CoCl<sub>2</sub> was added to the bath. This procedure suppressed  $I_{Ca}$ . In *C*,  $1 \mu M$ -TTX was added to the bath solution to block  $I_{Na}$ . Temperature  $32^\circ C$ ;  $5$  kHz low-pass filter.

with intracellular Cs<sup>+</sup> and TEA (see Methods). Fig. 3*A* shows a series of superimposed voltage-clamp records taken at a holding potential of  $-70$  mV, with depolarizing pulses of  $-30$  to  $+60$  mV. The initial peak currents show the typical pattern of Hodgkin-Huxley-type activation and inactivation of  $I_{Na}$ , and were completely suppressed by TTX. Note in Fig. 3*A* that current was still flowing more than  $10$  ms

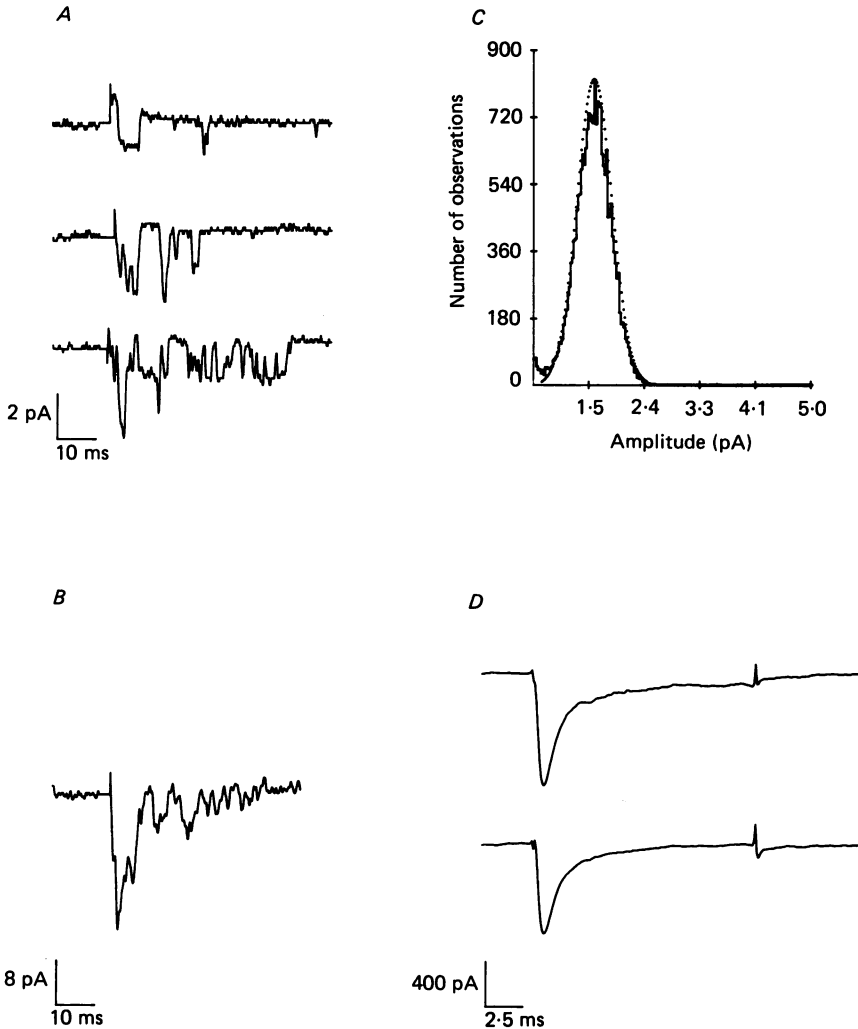


Fig. 4. Whole-cell  $I_{\text{Na}}$  compared to single-channel currents ( $i_{\text{Na}}$ ). *A*, single-channel currents in an outside-out patch.  $V_{\text{H}} = -70$  mV;  $V_{\text{C}} = -10$  mV. The time of the voltage step is indicated by the small positive-going capacitance artifacts. Only single openings are present in the top trace while the bottom two traces have double openings immediately after the potential step. The pipette contained the  $\text{K}^+$  saline solution described in the Methods but with  $\text{KF}$  substituted for  $\text{KCl}$  and no added  $\text{CaCl}_2$  or EGTA. The bath contained  $\text{Na}^+$  saline with  $\text{Ca}^{2+}$  replaced by  $3 \text{ mM-Co}^{2+}$ .  $2 \text{ kHz}$  low-pass filter. Temperature  $33^\circ\text{C}$ . *B*, the summation of sixteen sequential records (1024 points each) of single  $\text{Na}^+$ -channel traces including those seen in *A*. *C*, amplitude histogram of the openings of  $i_{\text{Na}}$ . Only sweeps with openings to a single channel level were analysed. The dotted line represents a Gaussian distribution fit to the data. *D*, whole-cell  $I_{\text{Na}}$  from a different cell than in *A-C* above but with the same bath solution, holding potential, command potential and temperature. The top trace is the current from a single sweep while the bottom trace is the average of sixteen sweeps after leakage current subtraction. The pipette was filled with the  $\text{Cs}^+$ -TEA solution (see Methods for composition).  $5 \text{ kHz}$  low-pass filter.

after the voltage step. By this time, current was presumptively carried by  $\text{Ca}^{2+}$ . This could be directly demonstrated by adding  $\text{Co}^{2+}$  or TTX to the bath to isolate  $I_{\text{Na}}$  and  $I_{\text{Ca}}$ , respectively (Fig. 3*B* and *C*). The inward current resistant to TTX was identified as  $I_{\text{Ca}}$  based on its well-known properties (Hagiwara, 1983): the current was blocked in a  $\text{Ca}^{2+}$ -free solution containing 3 mM- $\text{Co}^{2+}$  (Figs. 3*B* and 9), enhanced in a solution in which extracellular  $\text{Ca}^{2+}$  was replaced by equimolar or less  $\text{Ba}^{2+}$  (Fig. 9), and unaffected by high concentrations (40  $\mu\text{M}$ ) of TTX (not illustrated).

The rates of activation and inactivation were obviously slower for the  $\text{Ca}^{2+}$  than for the  $\text{Na}^+$  component. In solitary retinal ganglion cells the time course of  $I_{\text{Na}}$  could be fitted approximately by the sum of two exponentials (neglecting initial delays). For example, at 32 °C a step from  $-90$  to  $-15$  mV resulted in an activation time constant of  $0.10 \pm 0.03$  ms (means  $\pm$  s.d.) and an inactivation time constant ( $\tau_{\text{h}}$ ) of  $0.66 \pm 0.04$  ms ( $n = 5$ ). Following the kinetic analysis of Fenwick, Marty & Neher (1982*b*), the rising phase of  $I_{\text{Ca}}$  could be approximately fitted by the sum of two exponential components: a major slow component ( $\tau_1$ ) and a faster component ( $\tau_2$ ) of the opposite polarity. The faster component was necessary in order to account for the delay in the rising phase of  $I_{\text{Ca}}$  following the voltage stimulus. This finding is consistent with a multiple-step model for activation of  $I_{\text{Ca}}$ . Under the same conditions as for the  $I_{\text{Na}}$  activation kinetics described above,  $\tau_1$  was  $0.87 \pm 0.05$  ms and  $\tau_2$  was  $0.25 \pm 0.04$  ms ( $n = 4$ ) for the rising phase of  $I_{\text{Ca}}$ . Inactivation of  $I_{\text{Ca}}$  occurred over several seconds, and in some cells  $I_{\text{Ca}}$  was present more than 10 s after the initial depolarizing pulse. In response to each voltage pulse, only a relatively sustained  $I_{\text{Ca}}$  was observed in these mammalian retinal ganglion cells, although it remains possible that there is more than one class of  $\text{Ca}^{2+}$  current as in some other excitable cells (Carbone & Lux, 1984; Nowycky, Fox & Tsien, 1985).

With time, whole-cell  $I_{\text{Ca}}$  exhibited a marked decline in amplitude ('rundown'). For this reason the kinetics of the current and the properties of the tail current were not analysed in detail. During these experiments, the time constant of the decay of the capacitive current was monitored shortly after forming a whole-cell recording and again later after measuring  $I_{\text{Ca}}$ . In all cells analysed this time constant was less than 50  $\mu\text{s}$ . This ensured that the pipette tip was large enough to allow the rapid equilibrium of its small molecules with those of the cell (Fenwick *et al.* 1982*a, b*). Thus, any cytoplasmic component within the cell that is necessary for normal  $\text{Ca}^{2+}$ -channel function would have been quickly and irreversibly diluted. The rate of half-deterioration of the  $\text{Ca}^{2+}$  current varied from cell to cell (range  $\sim 30$  s to 15 min,  $n = 21$ ).

Fig. 4*A* shows single-channel records of  $i_{\text{Na}}$  obtained from isolated, outside-out patches. In the lower two traces two channels were occasionally open at the same time. These channels were blocked by 0.1  $\mu\text{M}$ -TTX (not illustrated). The unitary current was about  $-1.5$  pA, as judged from amplitude histograms similar to that in Fig. 4*C*. Fig. 4 also compares some properties of whole-cell  $I_{\text{Na}}$  to single-channel  $i_{\text{Na}}$ . Although the sum of the single-channel  $i_{\text{Na}}$  traces qualitatively resembled the 'macroscopic' whole-cell  $I_{\text{Na}}$  (compare Fig. 4*B* and *D*), there were notable quantitative differences, especially in the inactivation phase. For example, in Fig. 4*B*  $\text{Na}^+$  current was present more than 10 ms after the onset of the depolarizing stimulus. This was evident even when only a few single-channel records were averaged. In part

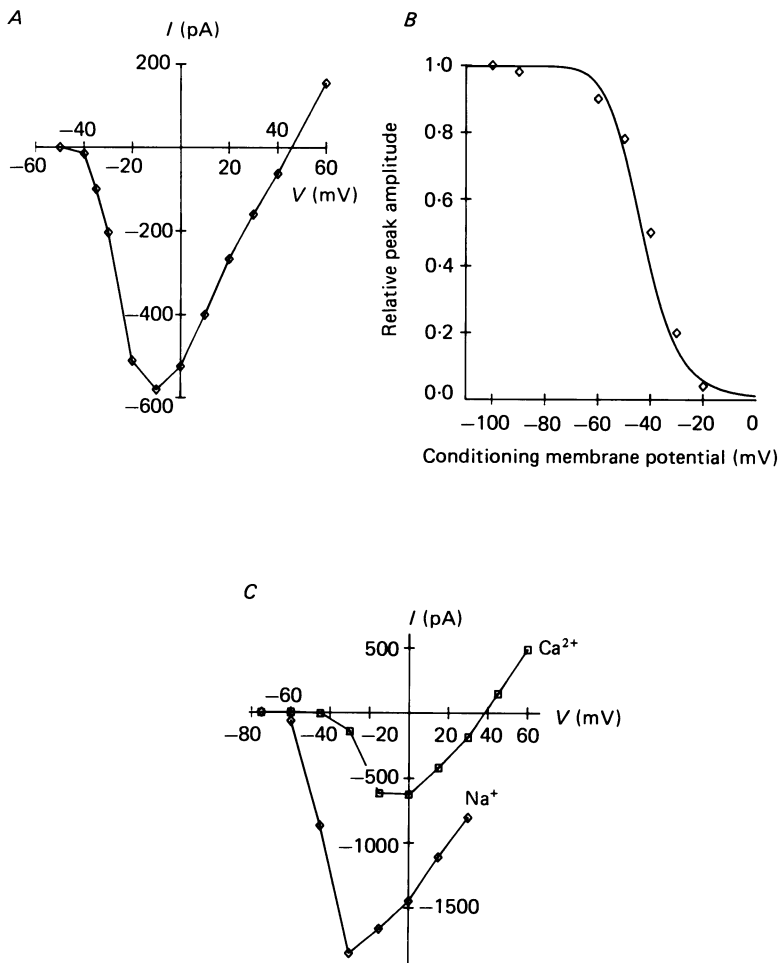


Fig. 5. Analysis of  $I_{Na}$  and  $I_{Ca}$  from whole-cell recordings. *A*, plot of peak  $I_{Na}$  amplitude against test voltage. Prior to depolarization to the test potential, the cell was held at  $-70$  mV. *B*, inactivation curve of  $I_{Na}$ . The cell was initially held at  $-70$  mV. Then a conditioning pre-pulse, whose amplitude is represented on the abscissa, was applied for 25 ms in order to reach a steady-state of inactivation prior to a final test pulse to  $-10$  mV. The peak amplitude of the current during the test pulse was normalized to the maximal value (attained when the conditioning pulse was  $-100$  mV), and this current was found to inactivate as the conditioning pulse became more depolarized. For both *A* and *B* the bath contained  $Na^+$  saline with  $Ca^{2+}$  replaced by  $3$  mM- $Co^{2+}$ , and the pipette the  $Cs^+$ -TEA solution; same cell as in Fig. 4*D*. *C*,  $I$ - $V$  relationships for  $I_{Na}$  ( $\diamond$ ) and  $I_{Ca}$  ( $\square$ ) calculated from the ganglion cell responses in Fig. 3*B* and *C*. Peak levels of current are plotted against the voltage stimulus. The apparent reversal potential of  $I_{Ca}$  was about  $+40$  mV. However, the calculated reversal potential for  $0.2$   $\mu$ M-internal  $Ca^{2+}$  and  $2.5$  mM-external  $Ca^{2+}$  is  $+120$  mV, so the outward current at voltages just positive to the reversal potential cannot be comprised of  $Ca^{2+}$ . This charge may be carried by monovalent ions such as  $Cs^+$  which may permeate  $Ca^{2+}$  channels during strong depolarizations (Fenwick *et al.* 1982*b*; Lee & Tsien, 1982).

this difference may have been secondary to changes in the ionic milieu since  $F^-$  rather than  $Cl^-$  was used as the major internal anion (Chandler & Meeves, 1970) in order to increase the stability of the outside-out patches.

Another difference between the single-channel  $i_{Na}$  and whole-cell  $I_{Na}$  was an apparent shift of the current-voltage ( $I-V$ ) relationships. However, no difference was present if the whole-cell recording lasted more than 15 min before an outside-out patch was formed. This phenomenon occurred because the whole-cell  $I-V$  relation slowly shifted in a hyperpolarizing direction to a new equilibrium during this time period, possibly reflecting internal dialysis with the solution in the pipette. In Fig. 5A the peak amplitude of whole-cell current is plotted against test pulse level ( $I-V$  curve) in an experiment in which  $Co^{2+}$  replaced extracellular  $Ca^{2+}$ . Presumably, therefore, only  $I_{Na}$  was measured. The maximum inward current of nearly  $-600$  pA was reached at  $-10$  mV. In cells of comparable size the peak inward current ranged from about  $-250$  to  $-2000$  pA. The ganglion cell used for the recordings of Fig. 5A lacked processes, was nearly spherical, and had a diameter of  $16 \mu m$ ; the capacitance of the cell was  $7.2$  pF. Therefore, for this cell the maximum inward current density was  $75 \mu A/cm^2$ , and the geometric capacitance,  $0.9 \mu F/cm^2$ . At this potential ( $V_C = -10$  mV) the unitary current ( $i_{Na}$ ) was about  $-1.5$  pA (Fig. 4C); but, from ensemble fluctuation analysis, only about 50% of the channels were open at the maximum peak current (S. A. Lipton, unpublished observations; Fenwick *et al.* 1982b; Sigworth, 1980). Using these estimates, this cell had a  $Na^+$  channel density of about 1 channel/ $\mu m^2$  or 800 channels per cell. This density would have to be corrected slightly for the effect of ultraslow inactivation (cf. Fenwick *et al.* 1982b).

Fig. 5B shows that another property of  $I_{Na}$ , inactivation of the whole-cell current, was similar to that seen by Hodgkin & Huxley (1952) with a potential of half-inactivation of about  $-40$  mV.

The  $I-V$  relationships for  $I_{Na}$  and  $I_{Ca}$  from the same solitary retinal ganglion cell are compared in Fig. 5C. Under the specified recording conditions, peak  $I_{Na}$  was greater than peak  $I_{Ca}$ . This observation held even when  $I_{Ca}$  was measured early in the recording period, presumably before significant rundown had occurred.

Taken together, the intracellular recordings along with the whole-cell or single-channel patch-pipette experiments leave little doubt that the action potentials measured in the soma of retinal ganglion cells contain both  $Na^+$  and  $Ca^{2+}$  components. Moreover, the conventional technique of intracellular recording and newer method of patch clamping yield complementary and generally concordant evidence about these conductances.

#### Whole-cell outward $K^+$ currents

By employing a protocol of pharmacological reagents and voltage pre-pulses during whole-cell recording with patch pipettes, three distinct  $K^+$  conductances could be distinguished. The currents resembled  $I_K$ ,  $I_A$  and  $I_{K(Ca)}$  of other preparations. In order to study each  $K^+$  current in isolation, other currents were suppressed. For example,  $I_{Na}$  was blocked by TTX while  $I_{Ca}$  was minimized by either permitting time for rundown (as in Fig. 6) or adding 3 mM- $Co^{2+}$  to the bath solution (as in Fig. 7C and D). These latter two procedures also decreased  $I_{K(Ca)}$ . Fig. 6A shows outward

current in response to depolarizing voltage steps in the presence of  $0.1 \mu\text{M}$ -TTX. This current appears to have a peak and a plateau.

*Effects of TEA on outward currents.* The addition of 20 mM-TEA decreased the early-peak current only slightly but greatly reduced the delayed-plateau current (Fig. 6*b*). The computer subtraction in Fig. 6*D* represents the TEA-suppressed

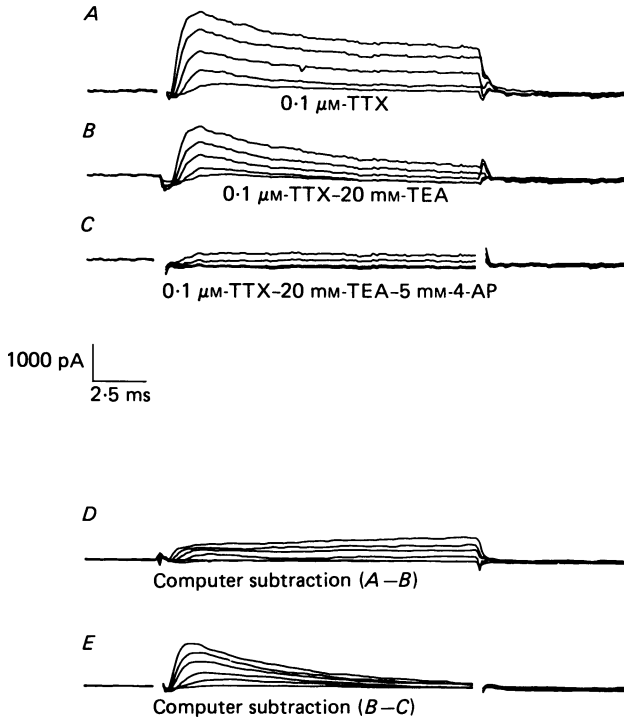


Fig. 6. Whole-cell recording of outward currents affected by TEA and 4-AP. A series of voltage steps was applied to a retinal ganglion cell. *A-C*, a single cell was superfused with  $0.1 \mu\text{M}$ -TTX (*A*),  $0.1 \mu\text{M}$ -TTX and 20 mM-TEA (*B*), or  $0.1 \mu\text{M}$ -TTX, 20 mM-TEA and 5 mM-4-AP (*C*). Steps were made from  $V_H = -90$  mV to command steps ( $V_C$ ) of  $-30$  to  $+30$  mV in 15 mV increments. *D* and *E*, computer subtractions of current records to display the current suppressed by TEA (*D*) and by 4-AP (*E*). These cases show  $V_C = -45$  to  $+30$  mV.  $I_{Ca}$  was allowed to run down (as evidenced by the absence of inward current in the presence of TTX, TEA and 4-AP) before these records were obtained. In some cases capacitive artifacts have been removed from the traces. Temperature  $33^\circ\text{C}$ ; 5 kHz low-pass filter.

current. This outward current increased with depolarizations above the resting potential, rose sigmoidally to a peak, and inactivated with a slow time constant compared to its activation. These properties are similar to those of the delayed outward current,  $I_K$  (Hodgkin & Huxley, 1952; Connor & Stevens, 1971*a*; Thompson, 1977). At some voltages, however, a transient component to the current is also discernible because of relaxation from an early peak (for example, the fourth step from the top in Fig. 6*D*). These findings are consistent with those in other neurones

in which externally applied TEA blocks  $I_K$  to a large extent and the transient current ( $I_A$ ) to a lesser degree (Thompson, 1977).

*Effects of 4-aminopyridine on outward currents.* When 5 mM-4-aminopyridine (4-AP) was added to the TTX and TEA, the transient component of the outward current disappeared (Fig. 6C). Fig. 6E is the computer subtraction to reveal the current suppressed by 4-AP. This current peaked rapidly (within 1.8 ms) and also inactivated quickly (in tens of milliseconds). This transient outward current resembles  $I_A$  previously studied in detail in other nerve cell bodies (Connor & Stevens, 1971c; Thompson, 1977). The time course of inactivation of  $I_A$  in other neurones can be fitted by a single exponential (Connor & Stevens, 1971B). Similarly, the decay of the transient current in retinal ganglion cells could be fitted by a single exponential. For example, Fig. 7A shows that for a step from a holding potential of  $-90$  mV to a command potential of  $+30$  mV, the current inactivated with a time constant of 6.8 ms. This time constant is fast compared to that found in gastropod neurones (Connor & Stevens, 1971b), as it is in other mammalian neurones (Belluzzi, Saachi & Wanke, 1985). The time constants in Fig. 7B also appeared to be voltage dependent, as in rat sympathetic neurones (Belluzzi *et al.* 1985). In addition,  $I_A$  can be completely inactivated by a depolarizing pre-pulse to  $-40$  mV (Connor & Stevens, 1971b). In Fig. 7D compared with 7C, after a 2 s pre-pulse to  $-40$  mV, the retinal ganglion cell had no remaining transient outward current. The delayed outward current was also decreased, but only by about a half. This finding is consistent with the notion that the delayed outward current is similar to the  $I_K$  of other neurones which has a half-maximal steady-state inactivation at about  $-40$  mV (Connor and Stevens, 1971a).

*I-V relationships of  $I_A$  and  $I_K$ .* *I-V* curves could be constructed for both the transient outward ( $I_A$ -type) and delayed outward ( $I_K$ -like) currents in retinal ganglion cells by taking advantage of their differential drug sensitivities and temporal properties. For example, Fig. 8A contains the *I-V* relationship of the peak transient currents in Fig. 6E. The shape of the *I-V* curve is typical for  $I_A$  (Connor & Stevens, 1971b). Since  $I_A$  had inactivated within 60 ms of depolarization, the *I-V* curve for the delayed outward component of the current could be constructed from the steady-state levels at the end of longer steps as in Fig. 7C. This *I-V* relationship is also plotted in Fig. 8A.

*K<sup>+</sup> selectivity of the outward currents.* Tail currents were observed when the cell was repolarized, during activation, to a new potential level. Fig. 8B shows that when the tail currents were measured at a time when  $I_K$  and  $I_A$  were coexistent, the data suggested relative selectivity for  $K^+$ . Tail currents obtained at times when either  $I_A$  or  $I_K$  was predominant yielded similar results (not illustrated). Since the concentration of  $Cl^-$  was equimolar on both sides of the membrane, the negative equilibrium potential of the tail current precludes  $Cl^-$  as the predominant permeant ion. The reversal potential of  $-68.4$  mV in this Figure is consistent with a channel selectivity that is predominantly (although perhaps not exclusively) for  $K^+$ ; the predicted reversal potential of a channel permeable solely to  $K^+$  is  $-82.6$  mV from the Nernst equation ( $35^\circ C$ ; external  $[K^+] = 5.84$  mM; internal  $[K^+] = 140$  mM). The *I-V* relationship of the tail current measured at the beginning of test pulses depended on external  $K^+$  concentration. The reversal potential shifted by  $+12$  mV in 10 mM-

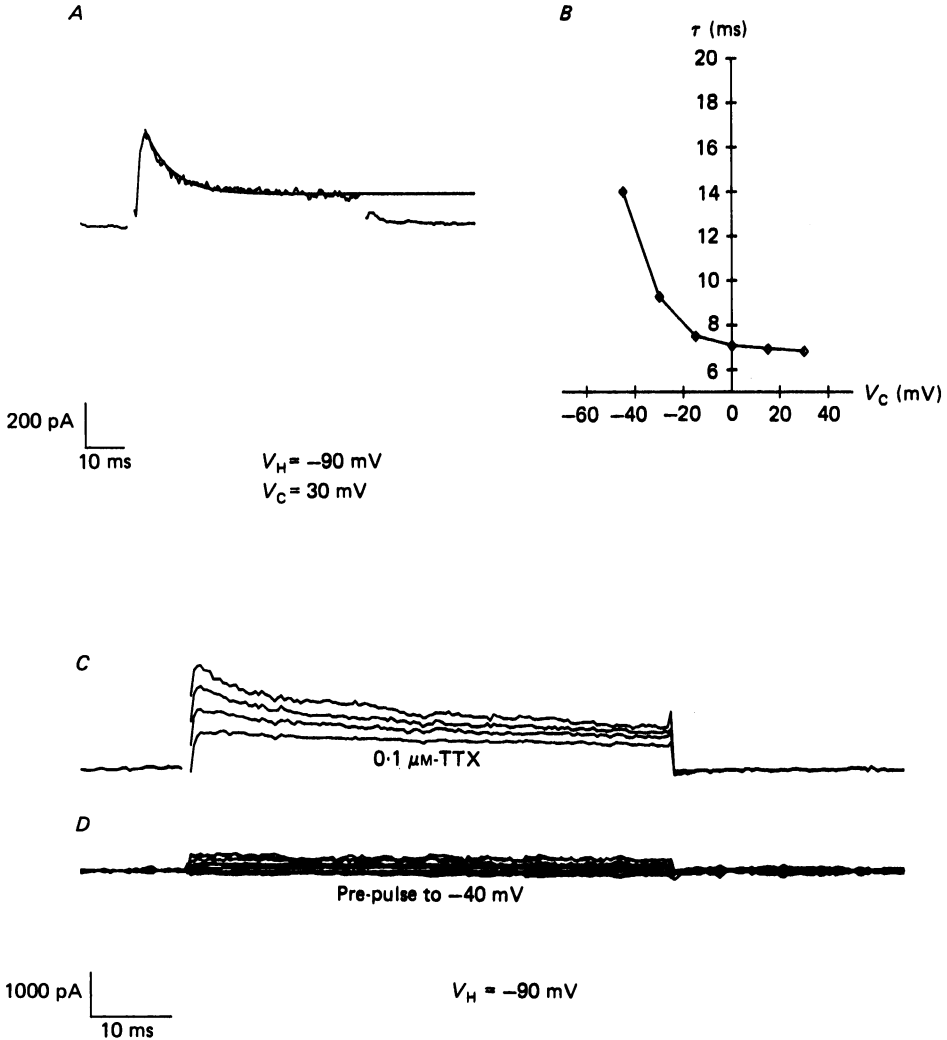


Fig. 7. Properties of  $I_A$  in a solitary rat retinal ganglion cell. *A* and *B*, decay of  $I_A$ . *A*, 4-AP-suppressible current obtained by computer subtraction as in Fig. 6*E*.  $V_H = -90$  mV;  $V_C = +30$  mV. The decay of the current was fitted by a single exponential with a time constant of 6.8 ms. *B*, similar exponential fits could be constructed for the decay of the currents elicited by  $V_C = -45$  to  $+30$  mV. These time constants ( $\tau$ ) are plotted against the command potential  $V_C$ . *C* and *D*, effect of a depolarizing pre-pulse on the transient outward ( $I_A$ ) and delayed outward ( $I_K$ ) currents. *C*, voltage steps were applied from  $V_H = -90$  to  $V_C = -15$  to  $+30$  mV in 15 mV increments. The outward currents elicited by these stimuli in the presence of 0.1  $\mu$ M-TTX are shown. The outward current had a transient peak and a more sustained delayed component. *D*, the voltage steps were applied from  $V_H = -90$  mV with a pre-pulse of 2 s duration to  $-40$  mV.  $V_C = -90$  to  $+30$  mV. The transient outward current ( $I_A$ ) was completely suppressed, and the delayed outward current ( $I_K$ ) was decreased by about 50%. Note also that under these conditions hyperpolarizing pulses following the pre-pulse elicited only a small inward current. The data in *A* and *B* and in *C* and *D* were collected from similar-appearing but different cells. The solutions, filtering, temperature and other parameters were the same as in Fig. 6 for *A* and *B*; in *C* and *D*,  $Ca^{2+}$  in the superfusion media was replaced by 3 mM- $Co^{2+}$  to block residual  $I_{Ca}$  and  $I_{K(Ca)}$ .

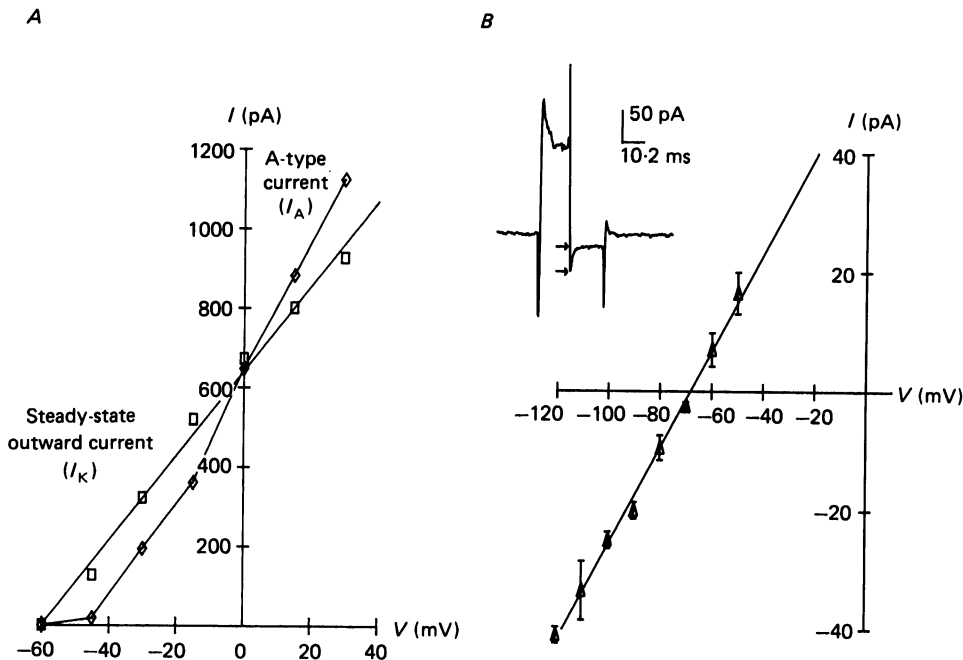


Fig. 8.  $I$ - $V$  relationships of  $I_A$ ,  $I_K$  (*A*) and of tail currents (*B*). *A*, peak currents ( $\diamond$ ) from Fig. 6*C* are plotted against the command potential to yield the  $I$ - $V$  curve for A-type current ( $I_A$ ). The shape of the curve is nearly identical to that for  $I_A$  in other cell types under relatively similar ionic conditions (Connor & Stevens, 1971*b*). Peak outward current increases rapidly as the membrane potential is depolarized above  $-50$  mV. The steady-state outward current level ( $\square$ ) for  $I_K$  was measured just before the end of the voltage steps shown in Fig. 7*C*. By this time  $I_A$  had inactivated. The line was fitted by least squares to the points with a correlation coefficient  $r^2 = 0.997$ . *B*, to measure the reversal potential for these currents, a double-pulse experiment was performed in a different cell.  $I_{Ca}$  was allowed to run down before recording  $K^+$  tail currents.  $V_H$  was  $-60$  mV. Activating command pulses (duration 15 ms) to  $+10$  mV were followed by voltage steps to  $-120$  to  $-50$  mV in 10 mV increments for 15 ms at  $\sim 1$  Hz. The tail current (measured between the arrows) for the voltage step to  $-120$  mV is shown in the inset (5 kHz low-pass filter; temperature  $32^\circ\text{C}$ ). Each data point ( $\triangle$ ) on the  $I$ - $V$  curve is the mean  $\pm$  s.d. for three determinations. The tail current reversed its polarity between  $-60$  and  $-70$  mV. A least-squares fit to the data points of the tail current  $I$ - $V$  curve had a correlation coefficient  $r^2 = 0.993$  and a reversal potential  $V_{rev} = -68.4$  mV.

external  $[K^+]$  ( $n = 3$ ), which approximates the value predicted from the Nernst equation ( $+14$  mV) for a channel that is permeable mainly to  $K^+$ .

*Whole-cell  $I_{K(Ca)}$ .* A presumptive  $I_{K(Ca)}$  could also be observed in retinal ganglion cells. In cells studied soon after a whole-cell recording was formed (and therefore prior to the rundown of  $I_{Ca}$ ), depolarizing voltage steps to  $+15$  or  $30$  mV evoked a transient inward current followed by a more slowly developing outward current ( $n = 12$ ). These currents were still observed in the presence of  $0.1 \mu\text{M}$ -TTX,  $20 \text{ mM}$ -TEA and  $5 \text{ mM}$ -4-AP (Fig. 9). Both the inward and outward currents, however, were blocked by  $3 \text{ mM}$ - $\text{Co}^{2+}$ . On the other hand,  $1 \text{ mM}$ - $\text{Ba}^{2+}$  substituted for  $2.5 \text{ mM}$ -external  $\text{Ca}^{2+}$  resulted in an enhanced inward current and no outward current.  $\text{Ba}^{2+}$  is

known to block many  $K^+$  channels and to carry larger currents through  $Ca^{2+}$  channels than  $Ca^{2+}$  itself (Alger & Nicoll, 1980; Hagiwara, 1983). Thus, one possibility is that the inward current was  $I_{Ca}$  and the outward current,  $I_{K(Ca)}$ . This interpretation is consistent with the previous one offered for the results of the conventional intracellular recordings (Fig. 1 D–F). There it was concluded that  $Co^{2+}$  or  $Ba^{2+}$ , but not

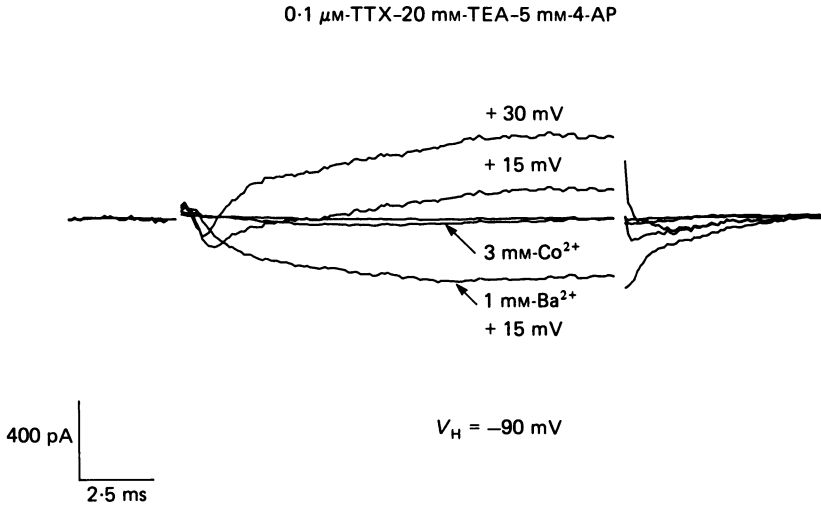


Fig. 9. Putative  $Ca^{2+}$  inward current followed by  $Ca^{2+}$ -activated outward current. A solitary ganglion cell was superfused with  $Na^+$  saline containing 0.1  $\mu M$ -TTX, 20 mM-TEA and 5 mM-4-AP. Unlike the data of Figs. 6–8, currents evoked by voltage steps here were measured immediately after forming a whole-cell recording, before  $I_{Ca}$  had run down. Steps from  $V_H = -90$  mV to  $V_C = +15$  or  $+30$  mV elicited inward followed by outward currents. The currents at both  $V_C$  levels were blocked by 3 mM- $CoCl_2$ . When 1 mM- $Ba^{2+}$  was substituted for the 2.5 mM- $Ca^{2+}$  in the  $Na^+$  saline bathing the cell, the peak inward current after a step to  $+15$  mV grew larger and the outward current was not observed. For clarity this current has been displaced slightly in time (0.45 ms to the right of the other traces in the record). The inward current in this Figure was most likely carried by  $Ca^{2+}$  while the outward current probably represented the  $Ca^{2+}$ -activated  $K^+$  conductance. The pipette contained  $K^+$  saline with  $2 \times 10^{-7}$  M- $Ca^{2+}$  (see Methods for composition). Temperature 33  $^{\circ}C$ ; 5 kHz low-pass filter.

TEA, completely blocked the after-hyperpolarization which was presumably mediated by a  $Ca^{2+}$ -activated  $K^+$  conductance. It is unlikely that the  $Ca^{2+}$ -activated outward current in Fig. 9 was carried by  $Cl^-$  instead of  $K^+$  because outward current was seen in some cells at the  $Cl^-$  equilibrium potential ( $V_C = 0$  mV). Under these conditions,  $I_{K(Ca)}$  was contaminated by inward  $I_{Ca}$ , which was technically unavoidable (Kaneko & Tachibana, 1985).

#### *Single-channel records of $K^+$ currents*

Conventional intracellular and whole-cell patch-electrode recordings suggested that  $I_{K(Ca)}$  was at least in part responsible for the after-hyperpolarization. Further evidence for this current in retinal ganglion cells has come from single-channel records using the patch-clamp technique. After forming a giga-ohm seal, depolarization of

membrane patches that were attached to the cell elicited large single-channel outward currents. With  $K^+$  saline in the pipette, the single-channel reversal potential in cell-attached patches was about 60 mV positive to rest (representing a true reversal potential of approximately 0 mV). In excised inside-out patches, these channels were relatively  $K^+$  selective, as evidenced by an extrapolated reversal potential from open

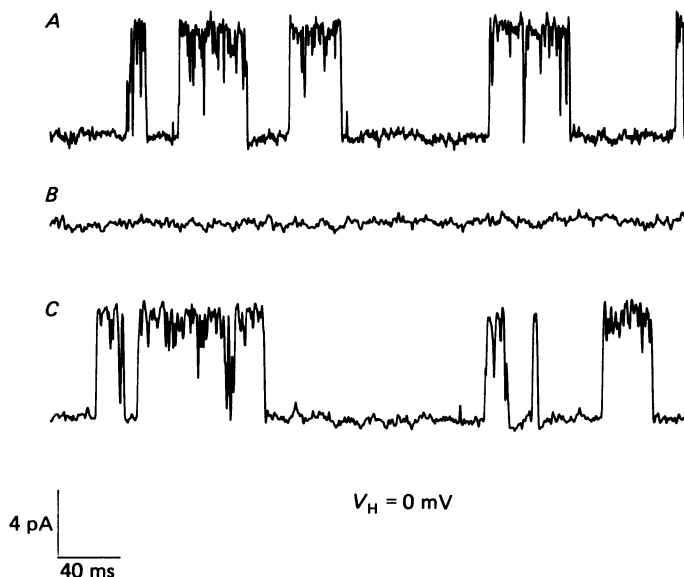


Fig. 10. Large single-channel  $K^+$  currents representing  $i_{K(Ca)}$ . *A*, an inside-out patch was bathed in the  $K^+$  saline solution and a Ca-EGTA buffer with a calculated free  $Ca^{2+}$  concentration of  $2 \times 10^{-7}$  M. No external potential was applied to the pipette which contained  $Na^+$  saline (see Methods for composition of the salines). Several large (7 pA) discrete  $K^+$  currents were seen (openings shown upward). *B*, changing the bath solution to contain 120 mM-CsCl and 20 mM-TEA (see Methods for complete composition) with  $2 \times 10^{-7}$  M-free  $Ca^{2+}$  resulted in the block of the channels. *C*, upon return of the  $K^+$  saline to the bath, the effect was reversible, and the channels began to open again. Temperature 34 °C; 2 kHz low-pass filter.

channel  $I-V$  curves of  $62.3 \pm 2.9$  mV (means  $\pm$  s.d.,  $n = 32$ ) in physiological solutions ( $Na^+$  saline on the external face of the membrane and  $K^+$  saline on the internal face), and  $0.2 \pm 1.1$  mV in symmetrical  $K^+$  solutions (see Methods for composition of these solutions). Also, the channels were not affected by the substitution of 2(*N*-morpholino) ethanesulphonic acid (MES) for  $Cl^-$  as the predominant anion. In agreement with similar channels in other tissues (Marty, 1981; Pallota, Magleby & Barrett, 1981; Barrett, Magleby & Pallotta, 1982; Maruyama, Gallacher & Petersen, 1983), the unitary conductance was large (about 115 pS at 34 °C in physiological solutions and 250 pS in symmetrical  $K^+$ ), openings were increased by depolarization, and the channels were blocked by an internal solution rich in  $Cs^+$  and TEA. For example, Fig. 10*A* shows single-channel currents in an excised inside-out patch held at a potential of 0 mV with  $K^+$  saline in the bath and  $Na^+$  saline in the pipette. In addition to several discrete openings and closings, the channel appeared to partially

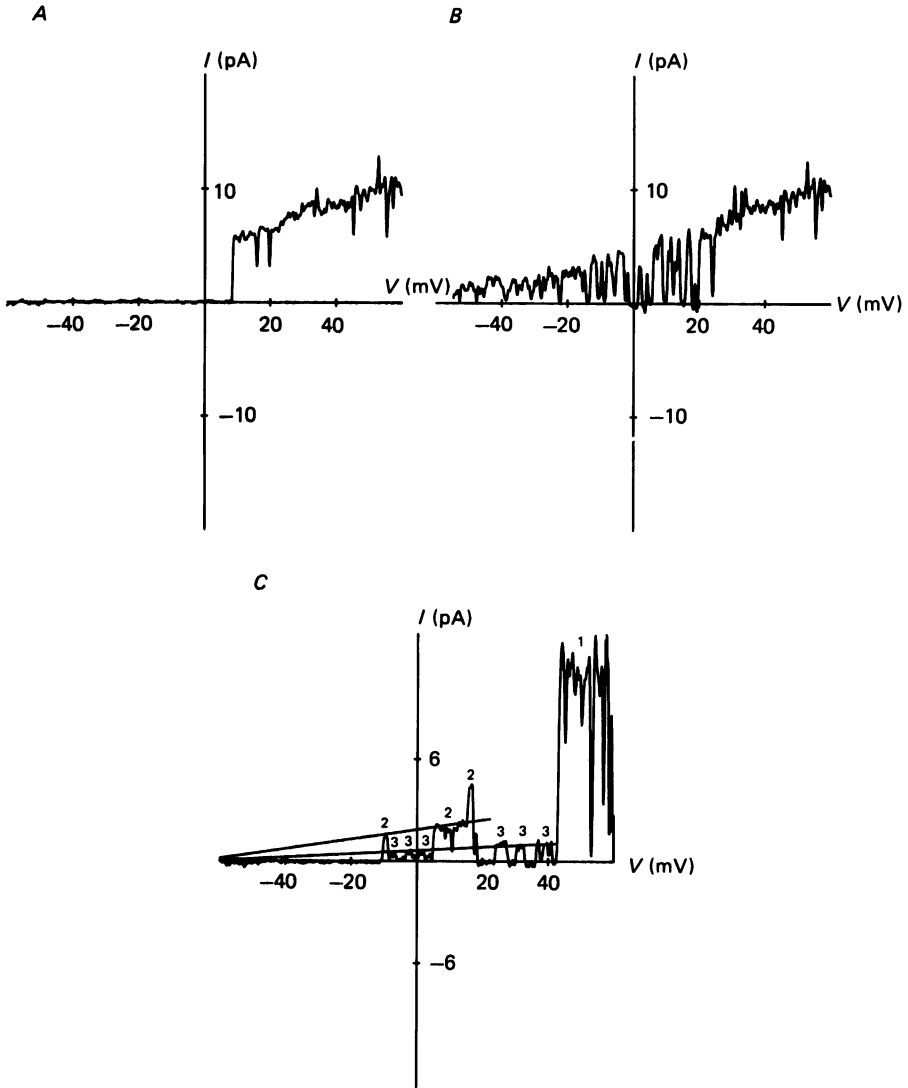


Fig. 11. For legend see opposite.

close or flicker during the longer openings. Obviously, at least some of these events may represent full closures that were not adequately resolved by the recording apparatus. Replacing the KCl in the bath with 120 mM-CsCl and 20 mM-TEA reversibly blocked the channel (Fig. 10*B* and *C*).

When a voltage ramp was applied to an inside-out patch displaying only a single large  $K^+$  channel (Fig. 11*A*), it became evident that the channel opened more frequently when depolarized. In sixty-four consecutive ramps the channel never opened below a potential of  $-10$  to  $0$  mV when the ramps began from the negative side. Voltage steps were used to prove that large depolarizations resulted in more frequent channel openings and increased fractional open times (not illustrated). In order to assess the reversal potential from the open-channel  $I-V$  curve, voltage ramps

were also applied in the opposite direction, i.e. starting from positive potentials. Thus, the channel would be likely to open when the ramp was initially applied (at a depolarizing level) and remain activated for a period sufficient to visualize the open state at progressively more negative potentials. Such an  $I$ - $V$  relationship is shown in Fig. 11 *B*. In this Figure, the channel begins to flicker between the open and closed states at potentials negative to +25 mV. A least-squares fit to the open level extrapolates to a reversal potential of -60.3 mV, as predicted for a relatively  $K^+$ -selective channel.

Occasionally when performing a ramp on some patches, other channels with smaller unitary conductances but with similar reversal potentials were observed (Fig. 11 *C*). None the less, these channel types were only rarely encountered (in six or fewer patches out of a total  $n = 201$ ). Fig. 11 *C* shows a single voltage-ramp trace that contained at least three types of channels with different conductances. Averaging the open state of each species of channel in several ramps from this inside-out patch revealed that all three channels had reversal potentials just negative to -60 mV (see legend for numerical values). All of these channels closed when a  $Cs^+$  and TEA solution was substituted for the  $K^+$  saline bathing the internal side of the membrane. The channel with the largest unitary conductance (the  $Ca^{2+}$ -activated  $K^+$  channel) was studied in detail here because it occurred in nearly every patch. Its  $K^+$  selectivity and voltage dependence were described above and its  $Ca^{2+}$  sensitivity, below. For the third largest of these channels (labelled 3 in Fig. 11 *C*), voltage steps in six inside-out patches revealed a unitary conductance of  $\sim 15$  pS at 30 °C, activation by depolarization, and relatively slow inactivation (Fig. 12). This behaviour is reminiscent of the delayed outward current ( $i_K$ ) which has a similar single-channel conductance and ionic selectivity in other cell types (DeCoursey, Chardy, Gupta & Cahalan, 1984; Ypey &

---

Fig. 11. Ramp clamps of relatively  $K^+$ -selective channels. A ramp potential was applied under voltage clamp. In *A* and *C*, single sweeps of the ramp clamp are shown after leakage subtraction using the method of Yellen (1982). *A*, an inside-out patch was excised in  $K^+$  saline with  $2 \times 10^{-7}$  M- $Ca^{2+}$  in the bath and  $Na^+$  saline in the pipette (see Methods for composition of these solutions). One large channel, representing  $i_{K(Ca)}$ , was observed in the patch. In this particular trace, the ramp began at -60 mV and the channel was closed until the potential reached +10 mV. For the duration of the ramp, it remained open except during some poorly resolved rapid or partial closings. *B*, current trace averaged from multiple ramps on the same inside-out patch as in *A*. Some  $K^+$  traces contributing to this composite were obtained with the potential beginning at +60 mV instead of at -60 mV in order to increase activation of the channel throughout the ramp. The line fitted to the open state of the channel by least squares had an extrapolated reversal potential  $V_{rev} = -60.3$  mV and a slope  $\gamma \simeq 100$  pS (fitted curve not shown). *C*, a different inside-out patch with three different channels of varying unitary conductance. The bath and pipette solutions were the same as in *A*. Each species of channel is numbered (1-3). Channel type 1 corresponded in unitary conductance to the large channel species observed in *A*. Note also that in this patch there were at least two channels of type 2. At +16 mV of the illustrated sweep, the second of the type 2 channels opened while the first one of the same type was already open. This was the only 'double opening' observed during this ramp. The open states of channel types 2 and 3 were reconstructed from multiple ramp sweeps (not shown) as described in Yellen (1982). The lines illustrated are the least-squares fit to these open states. From the lines, channel types 2 and 3 have  $V_{rev} = -63.1$  and -60.1 mV and  $\gamma = 30$  and 12 pS, respectively. All three of these ramps were filtered at 2 kHz. Temperature 30 °C.

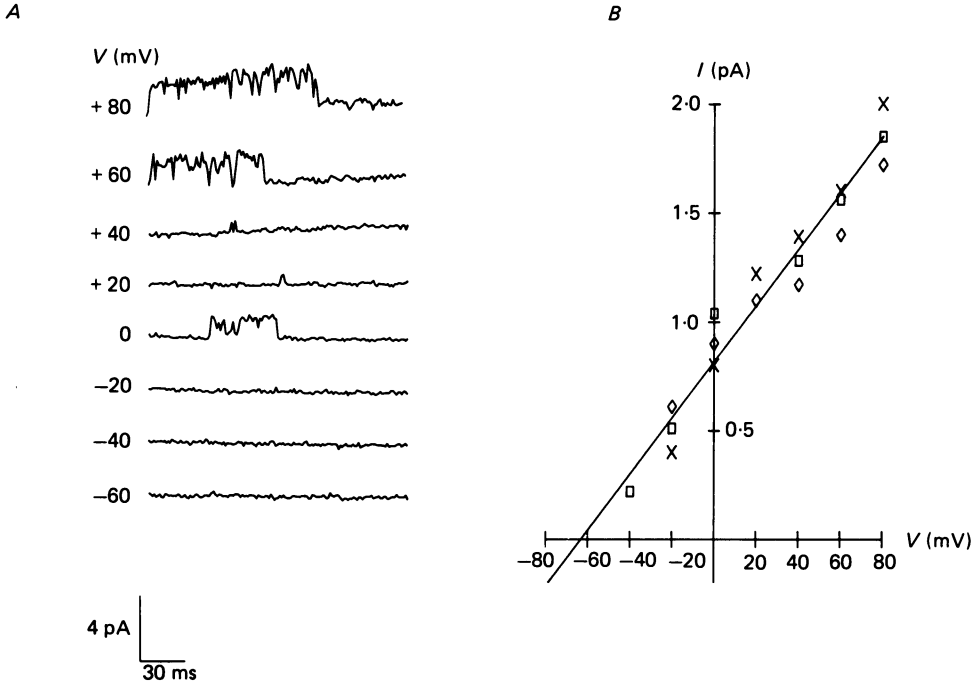


Fig. 12. Voltage dependence (*A*) and  $I$ - $V$  relationship (*B*) of a relatively  $K^+$ -selective channel with properties resembling the delayed outward-rectifying conductance in a solitary retinal ganglion cell. *A*, single-channel currents from an inside-out patch in response to depolarizing potential steps from a holding potential  $V_H = -80$  mV. The bath contained  $K^+$  saline with  $10^{-8}$  M- $Ca^{2+}$  and the pipette,  $Na^+$  saline (see Methods for compositions). 2 kHz low-pass filtering. Temperature  $30^\circ C$ . The amplitude of the channel was similar to that of the channel labelled 3 in Fig. 11*C*. Seven consecutive sweeps are shown that were obtained at a repetition rate of 0.8 Hz. As illustrated, although the channel was not activated with every voltage step, on average, it was more likely to open for longer durations with increasing depolarization. *B*, single-channel  $I$ - $V$  relation from three different inside-out patches for this channel, each represented by a different symbol.  $\square$  represents values obtained from the patch in *A*. The line illustrated was fitted by least squares to this data and has a slope  $\gamma = 13$  pS. It extrapolates to a reversal potential  $V_{rev} = 63.4$  mV. The other data could be fitted by lines with a  $\gamma = 16$  or  $12$  pS and a  $V_{rev} = -62.1$  or  $-65.3$  mV, respectively (fitted curves not shown).

Clapham, 1984). In these experiments the other type of channel with similar reversal potential (labelled 2 in Fig. 11*C*) was present in only three excised patches (total  $n = 201$  patches), precluding more than provisional characterization. This channel was transiently activated by depolarization ( $n = 3$ ), inactivated by pre-pulses to  $-40$  mV ( $n = 3$ ) and blocked by external 5 mM-4-AP ( $n = 2$ , in outside-out patches). Therefore, it is possible that this 30 pS channel represents the single-channel event underlying  $I_A$  observed during whole-cell recordings.

The dependence on internal  $Ca^{2+}$  concentration of the largest  $K^+$  channel (shown in Figs. 10, 11*A* and *B*, and as 1 in Fig. 11*C*) was studied in inside-out patches ( $n = 74$ ). When the  $Ca^{2+}$  concentration facing the internal side of the membrane was slowly raised from 0.2 to 18  $\mu M$ , the channels in the patch became vigorously active

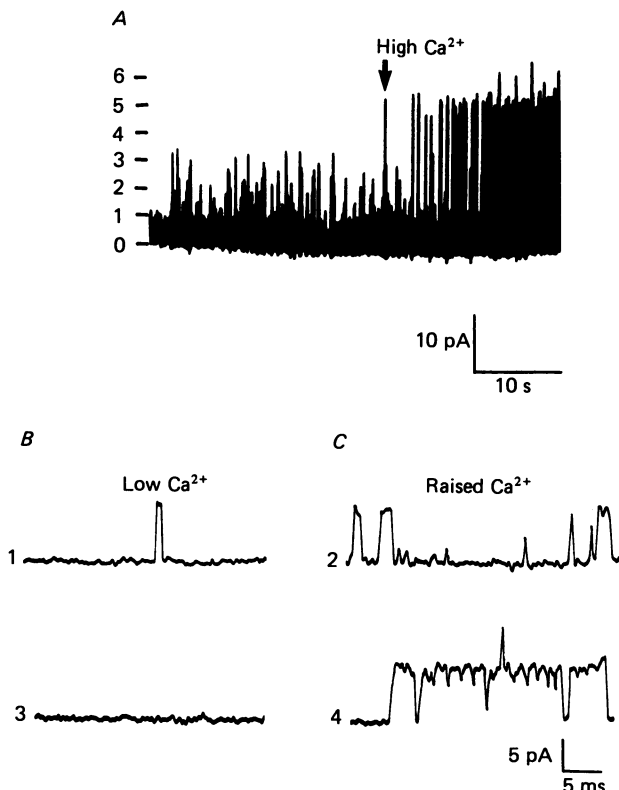


Fig. 13.  $\text{Ca}^{2+}$  activation of the large  $\text{K}^+$  channel. *A*, activation in a patch with many channels. An inside-out patch with at least seven of the largest species of  $\text{K}^+$  channels was initially bathed in  $\text{K}^+$  saline with  $0.2 \mu\text{M}$ - $\text{Ca}^{2+}$  at  $34^\circ\text{C}$ . The pipette contained  $\text{Na}^+$  saline (see Methods for composition of salines). Before the beginning of the trace, the membrane was stepped from  $-65$  to  $-20$  mV and held there. When the internal  $\text{Ca}^{2+}$  concentration was raised to  $18 \mu\text{M}$  (arrow at beginning of addition), an increasing number of channels opened. The scale on the left-hand side of the Figure represents the number of open channels. The single-channel activity was recorded with a Gould brush recorder,  $125$  kHz filtering. *B* and *C*,  $\text{Ca}^{2+}$  activation of discrete, single  $\text{K}^+$  channels in another inside-out patch. The activation by internal  $\text{Ca}^{2+}$  of the largest  $\text{K}^+$  channel was demonstrated in high-resolution traces of single channels. In each trace the membrane potential was held at  $+25$  mV. The pipette contained  $\text{Na}^+$  saline and the bath  $\text{K}^+$  saline (see Methods for compositions). For the traces in *B* the internal  $\text{Ca}^{2+}$  concentration was  $10^{-8}$  M and in *C*,  $2 \times 10^{-7}$  M. Each trace is typical of many obtained under similar conditions. In trace 1 (low  $\text{Ca}^{2+}$ ), channel openings were very infrequent. When the internal  $\text{Ca}^{2+}$  concentration was raised (trace 2), channel openings increased. Then the internal  $\text{Ca}^{2+}$  concentration was again lowered (trace 3), and the openings ceased. Finally, the  $\text{Ca}^{2+}$  concentration was raised (trace 4), and the openings increased again. Traces 2 and 4 also show two typical features of the kinetics of the  $\text{Ca}^{2+}$ -activated  $\text{K}^+$  channels: trace 2 – short bursts of channel openings with relatively long interburst intervals representing channel closures; trace 4 – long bursts of channel openings with short intraburst intervals, that in most cases appear as only partially resolved closings. This phenomenon has been called flicker between the open and closed states. Temperature  $31^\circ\text{C}$ ;  $2$  kHz low-pass filter.

(Fig. 13A). In another inside-out patch, internal  $\text{Ca}^{2+}$  concentration was repeatedly shuttled between 10 nM and 0.2  $\mu\text{M}$ . Under these conditions channel activity increased each time  $\text{Ca}^{2+}$  concentration was raised and decreased when it was lowered (Fig. 13B and C). Thus, with the patch-clamp technique  $\text{Ca}^{2+}$ -activated  $\text{K}^+$  channels were directly demonstrated after pharmacological evidence obtained with both conventional intracellular and whole-cell recordings had suggested their presence.

#### DISCUSSION

The detailed electrical properties of an identified, differentiated neurone from the mammalian C.N.S. have not been previously characterized in cultures from postnatal animals. For this purpose, ganglion cells were isolated from the rat retina, unequivocally identified with fluorescent probes, and cultured. Conventional intracellular and patch electrodes were used to document the presence of at least five voltage-dependent ionic conductances in solitary retinal ganglion cells: two inward currents carried by  $\text{Na}^+$  and  $\text{Ca}^{2+}$ , and three outward currents, all relatively selective for  $\text{K}^+$ . One  $\text{K}^+$  current resembled the delayed outward current (Hodgkin & Huxley, 1952; Connor & Stevens, 1971*a*; Thompson, 1977). Another  $\text{K}^+$  current had properties similar to the transient (A-type) current (Connor & Stevens, 1971*b*; Thompson, 1977; Belluzzi *et al.* 1985). The third  $\text{K}^+$  current was activated by a rise in internal  $\text{Ca}^{2+}$  concentration (Meech & Standen, 1975; Meech, 1978). All five currents could be activated by membrane depolarization.

Each current has been separated by a combination of its voltage dependence, time dependence, and sensitivity to mono- and divalent cations ( $\text{Cs}^+$ ,  $\text{Co}^{2+}$ , and  $\text{Ba}^{2+}$ ) as well as to specific drugs (TTX, TEA and 4-AP).  $I_{\text{Na}}$  was blocked by TTX without affecting the other currents and displayed classical Hodgkin-Huxley types of activation and inactivation.  $I_{\text{Ca}}$  could be suppressed by  $\text{Co}^{2+}$  (which did not influence  $I_{\text{Na}}$ ,  $I_{\text{K}}$  and  $I_{\text{A}}$ ) or, during whole-cell recording, by allowing for a period of time sufficient for the current to run down. An *internal* solution rich in  $\text{Cs}^+$  and TEA blocked all three  $\text{K}^+$  currents. Both  $I_{\text{K}}$  and  $I_{\text{A}}$  were sensitive to *external* TEA, but the former much more so than the latter (Fig. 6). The addition of 4-AP plus TEA to the extracellular bathing medium resulted in a much more complete suppression of  $I_{\text{A}}$ . Also,  $I_{\text{A}}$  could be completely inactivated by a pre-pulse to  $-40$  mV, which only approximately half-inactivated  $I_{\text{K}}$  (cf. Connor & Stevens, 1971*b*).  $I_{\text{K}}$  could be totally isolated from  $I_{\text{A}}$  by allowing  $I_{\text{A}}$  to inactivate with time (Fig. 7C).  $I_{\text{K(Ca)}}$  was *not* totally suppressed in the presence of 20 mM-TEA and 5 mM-4-AP (cf. Thompson, 1977). However,  $I_{\text{K(Ca)}}$  could be blocked together with  $I_{\text{Ca}}$  by  $\text{Co}^{2+}$ ; alternatively,  $I_{\text{K(Ca)}}$  could be blocked by  $\text{Ba}^{2+}$  which also carried more current through  $\text{Ca}^{2+}$  channels than  $\text{Ca}^{2+}$  itself. In an excised membrane patch  $i_{\text{K(Ca)}}$  could be isolated by holding the potential above  $-20$  mV and allowing the other currents to inactivate (Figs. 10 and 13). The blocking capability of extracellular TTX, TEA, 4-AP and  $\text{Co}^{2+}$  on their respective conductances must have been close to complete at the concentrations employed since the use of a combination of these agents resulted in only a small residual component (Fig. 9).

In the present study the pharmacology of the after-hyperpolarization and the whole-cell recordings of putative  $I_{\text{K(Ca)}}$  were identical in that both were eliminated in the presence of external

$Ba^{2+}$  and somewhat reduced by TEA (Figs. 1 and 9). We therefore tentatively conclude that this  $I_{K(Ca)}$  may underlie the after-hyperpolarization in mammalian retinal ganglion cells. The methods of the  $Ba^{2+}$  experiment cannot distinguish between the possibilities that  $Ba^{2+}$  is blocking the channels or not activating the current (in lieu of  $Ca^{2+}$  passing into the cell). In bull-frog sympathetic ganglion cells there are two types of  $Ca^{2+}$ -activated  $K^+$  currents, one of which ( $I_{a.h.p.}$ ) is blocked by external  $Ba^{2+}$  and is less sensitive to TEA (Pennefather, Lancaster, Adams & Nicoll, 1985). However, the time course of this current is quite prolonged and therefore entirely different from the  $I_{K(Ca)}$  studied here. In future experiments apamin may be useful in identifying the type of  $Ca^{2+}$ -activated current present in the whole-cell experiments since  $I_{a.h.p.}$  is irreversibly blocked by this toxin while the second type of  $Ca^{2+}$ -activated  $K^+$  current ( $I_C$ ) is not (Pennefather *et al.* 1985). In contrast,  $I_C$ -type current, mediated by the large-amplitude  $Ca^{2+}$ -activated  $K^+$  channels, is reversibly inhibited by charybdotoxin (Miller, Moczydlowski, Latorre & Phillips, 1985). Another possibility is that  $I_{K(Ca)}$  observed here may be a novel variant of this conductance that is present in the mammalian C.N.S.

To date, the solitary ganglion cells examined in culture in the present study are the only retinal neurones with definitive evidence for  $I_{Na}$  (for reference see Kaneko & Tachibana, 1985), although mammalian amacrine cells have yet to be investigated in this manner. Single-channel recordings in excised patches of membrane from these ganglion cells have directly confirmed the presence of  $Na^+$  as well as other types of ion channels. For example,  $Ca^{2+}$ -activated  $K^+$  channels were identified by their large unitary conductance, ionic selectivity, voltage dependence and internal  $Ca^{2+}$  concentration activation. These channels were presumed to underlie the macroscopic  $I_{K(Ca)}$ . Also, two channels with similar reversal potentials to  $i_{K(Ca)}$  but with smaller conductances occurred in these patches, albeit rarely (Figs. 11C and 12). They have yet to be encountered frequently enough to permit complete characterization, but from preliminary studies we speculate that they may underlie  $I_K$  and  $I_A$  observed during whole-cell recordings. On the other hand, two similar types of voltage-dependent  $K^+$  currents have been observed in bovine chromaffin cells (Marty & Neher, 1985) which do not show a macroscopic  $I_A$ ; the two smaller channels found in the present study that are relatively selective for  $K^+$  might resemble these channels.

The very low frequency of occurrence of these channels (in  $\leq 6$  of 201 patches) could reflect their low density in the membrane. As a first approximation of the number of channels present in the cell membrane that carry  $i_K$ , we can divide the whole-cell current ( $I_K$ ) at a particular voltage by the unitary current ( $i_K$ ) at that level. For example, at 0 mV  $I_K$  is 675 pA (from Fig. 8A) and  $i_K$  is about 0.9 pA (from Fig. 12). Thus, about 750 channels would be expected to be in the membrane, assuming the channel has a high probability of opening at that potential (if anything, this assumption should underestimate the number of channels). A similar calculation of  $I_A$  yields about 350 channels. The result of these estimates is similar in magnitude to that for  $Na^+$  channels, but  $Na^+$  channels were observed in about 50% of excised patches. Based upon these calculations, if the density of the  $K^+$  channels was uniform, we would have expected a higher yield of patches with these  $K^+$  channels. Other possibilities to account for this discrepancy include non-uniform distribution of channels in the membrane or lower probability of opening of these channels in excised patches than *in situ*.

In addition, during the course of the experiments of the present study,  $Cl^-$ -selective channels as well as non-selective cation channels were often observed in membrane patches from rat retinal ganglion cells. The non-selective cation channels (Lipton, 1985b) were similar to those reported in heart (Colquhoun, Neher, Reuter & Stevens, 1981) and in neuroblastoma (Yellen, 1982). Like the  $K^+$  channels with the largest

unitary conductance, the non-selective cation channels were also activated by internal  $\text{Ca}^{2+}$ , and openings increased in frequency in the period immediately following an action potential. Furthermore, the presence of multiple non-selective cation channels in most membrane patches from rat retinal ganglion cells has made the isolation of individual  $\text{Ca}^{2+}$  channels difficult, even with isotonic  $\text{Ba}^{2+}$  in the patch pipette. The detailed properties of both the  $\text{Cl}^-$ -selective and non-selective cation channels will be described elsewhere (S. A. Lipton, D. L. Tauck & E. Aizenman, in preparation).

Given the five voltage-dependent conductances described above, it seems possible to begin to interpret the transmembrane voltage recorded in mammalian retinal ganglion cells in response to injected current (Fig. 1A). Positive current pulses elicited action potentials followed by an after-hyperpolarization. Evidence has been obtained for the contribution of both  $\text{Na}^+$  and  $\text{Ca}^{2+}$  conductances to the action potential. The slow component of the action potential, observed with both intracellular and patch electrodes, appeared to be carried by  $\text{Ca}^{2+}$  since it was enhanced by raising external  $\text{Ca}^{2+}$  concentration or substitution with  $\text{Ba}^{2+}$ , blocked by  $\text{Co}^{2+}$  or  $\text{Cd}^{2+}$ , and not affected by TTX. The  $\text{Ca}^{2+}$  conductance was evident only in the presence of TEA which at least partially suppressed  $\text{K}^+$  currents. However,  $\text{Ca}^{2+}$  influx as well as voltage changes during the action potential may be of physiological importance in activating other conductances. Considering the period immediately following a spike, in gastropod neurones  $I_{\text{K}}$  dominates during repolarization while  $I_{\text{A}}$  predominates during the middle and latter interspike interval and thus plays a role in repetitive firing (Connor & Stevens, 1971c). In mammalian neurones, however, the time course of inactivation of  $I_{\text{A}}$  appears to be faster although the temperature is also higher (Fig. 7A and B, and Belluzzi *et al.* 1985). Thus, it may contribute to the repolarization phase of the action potential.  $\text{Ca}^{2+}$  entering during the action potential activates a  $\text{K}^+$  conductance which, along with  $I_{\text{K}}$ , is likely to contribute to the after-hyperpolarization. This pattern of conductances constitutes a negative feed-back system since an *inward*  $\text{Ca}^{2+}$  current triggers an *outward*  $\text{K}^+$  current that follows the action potential. Conceivably this feed-back system might influence the rate at which the cell reaches threshold and, therefore, modulate the frequency of spikes as well as exert a stabilizing effect on the membrane potential.

The use of both patch and micro-electrodes in the present study allowed comparison of the results obtained with the two techniques. Solitary ganglion cells in culture have resting potentials of about  $-60$  mV with either type of electrode. However, the input resistance of spatially compact cells measured with fine intracellular pipettes (250–300 M $\Omega$ ) was only one-third to one-tenth that obtained with patch electrodes filled with  $\text{K}^+$  saline (850 M $\Omega$  to 3 G $\Omega$ ). Fenwick *et al.* (1982a) reported a similar discrepancy for chromaffin cells and felt that the tighter seal of the patch pipette prevented leaking around the tip and provided more realistic values. Nevertheless, the change in intracellular milieu, engendered by internal dialysis of the cell with the solution in the patch electrode, could also affect the input resistance of the cell. For example, specific ionic conductances may be inactivated under these conditions, resulting in a higher input resistance. Another possible problem in comparing results obtained with intracellular and patch electrodes arises in the  $I$ - $V$  curves. The  $I$ - $V$  relationship for  $I_{\text{Na}}$  measured with a whole-cell voltage clamp shifted along the

abscissa in a hyperpolarizing direction during the first 15 min of recording, possibly reflecting the effects of internal dialysis (cf. Fernandez, Fox & Krasne, 1984). Also, for data obtained with the 'giga-seal' patch technique, the simple addition of the 'microscopic' single-channel currents in isolated patches did not always sum to an exact replica of the 'macroscopic' current from whole-cell recordings (e.g. for  $I_{Na}$  in Fig. 4). This discrepancy may possibly arise because of changes in composition at the internal face of the membrane. The internal milieu could be preserved by recording single-channel currents from cell-attached patches; without a second electrode, however, this technique does not permit absolute control of the transmembrane potential. For all of these reasons, it will continue to be important to compare results obtained from standard intracellular recording with those from the various configurations of patch-electrode recording.

Relatively few intracellular recordings have been made from mammalian retinal ganglion cells *in situ* (Wiesel, 1959; Nelson *et al.* 1978; Dacheux & Miller, 1981; Bloomfield & Dowling, 1985), apparently because of great difficulty in attaining stable penetrations of these cells with micro-electrodes. Therefore, it is not possible to correlate the results of the present paper with intracellular recordings *in situ*, except to state that membrane hyperpolarizations, depolarizations and action potentials had previously been found in response to light. However, extensive extracellular and optic nerve recordings have been performed in order to characterize the receptive field properties and chemical sensitivities of mammalian ganglion cells, for example, in the rabbit retina where there appear to be at least eighteen different types of ganglion cells (for a review see Daw *et al.* 1982). Several types of mammalian retinal ganglion cells have also been differentiated on anatomical grounds (for the cat, see Kolb *et al.* 1981). In cat (Kuffler, 1953; Enroth-Cugell & Robson, 1966; Cleland & Levick, 1974*a, b*; Stone & Fukada, 1974), rabbit (Barlow *et al.* 1964) and primates (Hubel & Wiesel, 1960), many retinal ganglion cells have in common a mutually antagonistic centre-surround organization of the receptive field; other properties vary and include sensitivity to direction, velocity, and orientation of image motion as well as local edge detection. For rat retinal ganglion cells electrophysiological measurements from optic nerve and tract have shown that the functional organization of one type of receptive field is concentrically arranged and similar to that in the above-mentioned mammals: Brown & Rojas (1965) found that the centre region responded to either an increase in light stimulation (on-response) or a decrease (off-response) while the larger concentric surround responded in an antagonistic fashion. In addition, both on- and off-centre units adapted to light either slowly or rapidly. However, in some rat retinal ganglion cells another type of receptive field organization was observed in which the surround region was not present (Brown & Rojas, 1965). No other types of receptive fields were encountered, but recording directly from retina rather than from optic nerve or tract may reveal more types of cells as it has in other mammals. Therefore, one should remain cautious and not conclude that the receptive fields of rat retinal ganglion cells have simpler properties than the other mammals studied.

Despite the electrophysiological evidence in the rat retina for at least two types of ganglion cells based upon receptive field properties, all of the cells recorded from in the present experiments ( $n \simeq 400$ ) displayed similar ionic conductances. This

finding makes it likely that the subclasses of rat retinal ganglion cells have these membrane currents in common. Alternatively, the dissociation procedure may have inadvertently selected for one type of ganglion cell. In rodents like those of the present study, there is a population of large ganglion cells which can be labelled with neurofibrillar stains and appear homologous to the  $\alpha$  or Y cells of the cat (Fukada, 1977; Perry, 1979; Dräger, Edwards & Barnstable, 1984). In addition, in rats small- and medium-sized ganglion cell bodies have also been encountered and may be analogous to the  $\delta$  and  $\gamma$  cells in the cat retina (Fukada, 1977; Perry, 1979). Using antibodies to the 145000 molecular weight neurofilament subunit, we have been able to unequivocally identify the class of large,  $\alpha$ -like ganglion cells in rat retinal cultures, and thus distinguish this population from the other ganglion cells labelled by retrograde transport but not by the antibody (Dräger, Edwards & Kleinschmidt, 1983; Dräger, Edwards & Barnstable, 1984; Dräger & Hofbauer, 1984; S. A. Lipton & U. C. Dräger, in preparation). The ability to distinguish at least two subclasses of ganglion cells in culture eliminates the possibility that the isolation procedure somehow selected for one particular class of ganglion cells. Therefore, it is our tentative conclusion that all retinal ganglion cell subtypes have the ionic currents described in the present paper, although the amplitude of each current appears to vary somewhat from cell to cell.

The characteristics of these several conductances could be altered by changes in membrane properties after dissociation of ganglion cells from the retina; but another possibility is that these measurements truly reflect the varied repertoire of ionic currents in these central neurones. Enzymically cleansed, solitary cells permit isolation and analysis of currents using the patch-clamp technique that is not feasible in the intact retina. By studying the effects of putative neurotransmitters on these conductances as well as on other chemically gated conductances (S. A. Lipton, D. L. Tauck & E. Aizenman, in preparation), their contribution to the functioning of the cell and its receptive field properties may begin to be deduced.

We thank Torsten Wiesel for encouragement and support, Matthew Frosch for discussions and computer programs, Dana Leifer for collaborating on the development of the cell culture system, Paul Harcourt and Micheal Phillips for technical assistance, and Marc Dichter and Elias Aizenman for reading the manuscript. This investigation was supported by NIH grants EY05477 and NS00879, by a Mary and Alexander P. Hirsch Award from Fight For Sight, Inc., New York City, to S. A. L. and post-doctoral fellowship NS07264 to D. L. T.

#### REFERENCES

- ALGER, B. E. & NICOLL, R. A. (1980). Epileptiform burst after-hyperpolarization: calcium-dependent potassium potential in hippocampal CA1 pyramidal cells. *Science* **210**, 1122–1124.
- ARIEL, M. & DAW, N. W. (1982*a*). Effects of cholinergic drugs on receptive field properties of rabbit retinal ganglion cells. *Journal of Physiology* **324**, 135–160.
- ARIEL, M. & DAW, N. W. (1982*b*). Pharmacological analysis of directionally sensitive rabbit retinal ganglion cells. *Journal of Physiology* **324**, 161–185.
- BADER, C. R., MACLEISH, P. R. & SCHWARTZ, E. A. (1979). A voltage-clamp study of the light response in solitary rods isolated from tiger salamander. *Journal of Physiology* **296**, 1–26.
- BARLOW, H. B., HILL, R. M. & LEVICK, W. R. (1964). Retinal ganglion cells responding selectively to direction and speed of image motion in the rabbit. *Journal of Physiology* **173**, 377–407.
- BARRETT, J. N., MAGELBY, K. L. & PALLOTA, B. S. (1982). Properties of single calcium-activated potassium channels in cultured rat muscle. *Journal of Physiology* **331**, 211–230.

- BELLUZZI, O., SAACHI, O. & WANKE, E. (1985). A fast transient outward current in the rat sympathetic neurone studied under voltage-clamp conditions. *Journal of Physiology* **358**, 91–108.
- BLOOMFIELD, S. A. & DOWLING, J. E. (1985). Roles of aspartate and glutamate on synaptic transmission in rabbit retina. II. Inner plexiform layer. *Journal of Neurophysiology* **53**, 714–725.
- BOLZ, J., FRUMKES, T., VOIGT, T. & WÄSSLE, H. (1985*a*). Action and localization of  $\gamma$ -aminobutyric acid in cat retina. *Journal of Physiology* **362**, 369–393.
- BOLZ, J., THIER, P., VOIGT, T. & WÄSSLE, H. (1985*b*). Action and localization of glycine and taurine in the cat retina. *Journal of Physiology* **362**, 395–413.
- BROWN, J. E. & ROJAS, J. A. (1965). Rat retinal ganglion cells: receptive field organization and maintained activity. *Journal of Neurophysiology* **28**, 1073–1090.
- CALDWELL, P. C. (1970). Calcium chelation and buffers. In *Calcium and Cellular Function*, ed. CUTHBERT, R. W., pp. 10–16. New York: St. Martin's Press.
- CARBONE, E. & LUX, H. D. (1984). A low voltage-activated fully inactivating Ca channel in vertebrate sensory neurones. *Nature* **310**, 501–502.
- CHANDLER, W. K. & MEEVES, H. (1970). Rate constants associated with changes in sodium conductance in axons perfused with sodium fluoride. *Journal of Physiology* **211**, 679–705.
- CLELAND, B. G. & LEVICK, W. R. (1974*a*). Brisk and sluggish concentrically organized ganglion cells in the cat retina. *Journal of Physiology* **240**, 421–456.
- CLELAND, B. G. & LEVICK, W. R. (1974*b*). Rarely encountered types of ganglion cells in the cat's retina and an overall classification. *Journal of Physiology* **240**, 457–492.
- COLQUHOUN, D., NEHER, E., REUTER, H. & STEVENS, C. G. (1981). Inward current channels activated by intracellular Ca in cultured cardiac cells. *Nature* **294**, 752–754.
- CONNOR, J. A. & STEVENS, C. F. (1971*a*). Inward and delayed outward membrane currents in isolated neural somata under voltage clamp. *Journal of Physiology* **213**, 1–19.
- CONNOR, J. A. & STEVENS, C. F. (1971*b*). Voltage clamp studies of a transient outward membrane current in gastropod neural somata. *Journal of Physiology* **213**, 21–30.
- CONNOR, J. A. & STEVENS, C. F. (1971*c*). Prediction of repetitive firing behaviour from voltage clamp data on an isolated neurone soma. *Journal of Physiology* **213**, 31–53.
- DACHEUX, R. F. & MILLER, R. F. (1981). An intracellular electrophysiological study of the ontogeny of functional synapses in the rabbit retina. II. Amacrine cells. *Journal of Comparative Neurology* **198**, 327–334.
- DAW, N. W., ARIEL, M. & CALDWELL, J. H. (1982). Function of neurotransmitters in the retina. *Retina* **4**, suppl., 322–331.
- DECOURSEY, T. E., CHARDY, K. G. GUPTA, S. & CAHALAN, M. D. (1984). Voltage-gated K<sup>+</sup> channels in human T lymphocytes: a role in mitogenesis? *Nature* **307**, 465–468.
- DOWLING, J. E. & BOYCOTT, B. B. (1966). Organization of the primate retina. *Proceedings of the Royal Society B* **166**, 80–111.
- DOWLING, J. E., PAK, M. W. & LASATER, E. M. (1985). White perch horizontal cells in culture: methods, morphology and process growth. *Brain Research* **360**, 331–338.
- DRÄGER, U. C., EDWARDS, D. L. & BARNSTABLE, C. J. (1984). Antibodies against filamentous components in discrete cell types of the mouse retina. *Journal of Neuroscience* **4**, 2025–2042.
- DRÄGER, U. C., EDWARDS, L. D. & KLEINSCHMIDT, J. (1983). Neurofilaments contain  $\alpha$ -melanocyte-stimulating hormone ( $\alpha$ -MSH)-like immunoreactivity. *Proceedings of the National Academy of Sciences of the U.S.A.* **80**, 6408–6412.
- DRÄGER, U. C. & HOFBAUER, A. (1984). Antibodies to heavy neurofilament subunit detect a subpopulation of damaged ganglion cells in retina. *Nature* **309**, 624–626.
- ENROTH-CUGELL, C. & ROBSON, J. G. (1966). The contrast sensitivity of retinal ganglion cells of the cat. *Journal of Physiology* **187**, 517–522.
- FENWICK, E. M., MARTY, A. & NEHER, E. (1982*a*). A patch-clamp study of bovine chromaffin cells and of their sensitivity to acetylcholine. *Journal of Physiology* **331**, 577–597.
- FENWICK, E. M., MARTY, A. & NEHER, E. (1982*b*). Sodium and calcium channels in bovine chromaffin cells. *Journal of Physiology* **331**, 599–635.
- FERNANDEZ, J. M., FOX, A. P. & KRASNE, S. (1984). Membrane patches and whole-cell membranes: a comparison of electrical properties in rat clonal pituitary (GH<sub>3</sub>) cells. *Journal of Physiology* **356**, 565–585.
- FUKADA, Y. (1977). A three-group classification of rat retinal ganglion cells: histological and physiological studies. *Brain Research* **119**, 327–344.

- GRANIT, R. (1955). Centrifugal and antidromic effects on ganglion cells of retina. *Journal of Neurophysiology* **18**, 388–411.
- HAGIWARA, S. (1983). *Membrane Potential-dependent Ion Channels in Cell Membrane. Phylogenetic and Developmental Approaches*. New York: Raven Press.
- HAGIWARA, S. & BYERLY, L. (1981). Calcium channel. *Annual Review of Neuroscience* **4**, 69–125.
- HAGIWARA, S. & NAKA, K. (1964). The initiation of spike potential in barnacle muscle fibres under low intracellular  $\text{Ca}^{2+}$ . *Journal of General Physiology* **48**, 141–162.
- HAMILL, O. P., MARTY, A., NEHER, E., SAKMANN, B. & SIGWORTH, F. J. (1981). Improved patch-clamp techniques for high-resolution current recording from cells and cell-free membrane patches. *Pflügers Archiv* **391**, 65–100.
- HODGKIN, A. L. & HUXLEY, A. F. (1952). A quantitative description of membrane current and its application to conduction and excitation in nerve. *Journal of Physiology* **117**, 500–544.
- HUBEL, D. H. & WIESEL, T. N. (1960). Receptive fields of optic nerve fibres in the spider monkey. *Journal of Physiology* **154**, 572–580.
- IKEDA, H. & SHEARDOWN, M. J. (1982). Acetylcholine may be an excitatory transmitter mediating visual excitation of 'transient' cells with the periphery effect in the cat retina: iontophoretic studies *in vivo*. *Neuroscience* **7**, 1299–1308.
- JENSEN, R. J. & DAW, N. W. (1984). Effects of dopamine antagonists on receptive fields of brisk cells and directionally sensitive cells in the rabbit retina. *Journal of Neuroscience* **4**, 2972–2985.
- KANEKO, A. & HASHIMOTO, H. (1968). Electrophysiological study of single neurones in the inner nuclear layer of the carp retina. *Vision Research* **9**, 37–55.
- KANEKO, A. & TACHIBANA, M. (1985). A voltage-clamp analysis of membrane currents in solitary bipolar cells dissociated from *Carassius auratus*. *Journal of Physiology* **358**, 131–152.
- KIRBY, A. W. & SCHWEITZER-TONG, D. E. (1981). GABA-antagonists alter spatial summation in receptive field centres of rod- but not cone-driven cat retinal ganglion Y-cells. *Journal of Physiology* **320**, 303–308.
- KOLB, H., NELSON, R. & MARIANA, A. (1981). Amacrine cells, bipolar cells and ganglion cells of the cat retina: a golgi study. *Vision Research* **21**, 1081–1114.
- KUFFLER, S. W. (1953). Discharge patterns and functional organization of mammalian retina. *Journal of Neurophysiology* **16**, 37–68.
- LASATER, E. M. & DOWLING, J. E. (1982). Carp horizontal cells in culture respond selectively to L-glutamate and its agonists. *Proceedings of the National Academy of Sciences of the USA* **79**, 936–940.
- LEE, K. S. & TSIEN, R. W. (1982). Reversal of current through calcium channels in dialysed single heart cells. *Nature* **297**, 498–501.
- LEIFER, D., LIPTON, S. A., BARNSTABLE, C. J. & MASLAND, R. H. (1984). Monoclonal antibody to Thy-1 enhances regeneration of processes by rat retinal ganglion cells in culture. *Science* **224**, 303–306.
- LIPTON, S. A. (1983). cGMP and EGTA increase the light-sensitive current of retinal rods. *Brain Research* **265**, 41–48.
- LIPTON, S. A. (1985a). Conditioning hyperpolarization reveals a property of the light-sensitive current in photoreceptors that is modified by cGMP and EGTA. *Brain Research* **341**, 337–349.
- LIPTON, S. A. (1985b). Presence of regenerating processes is associated with prolonged bursting of calcium-activated nonselective cation channels. *Neuroscience Abstracts* **11**, 177.
- LIPTON, S. A. (1986). Blockade of electrical activity promotes the death of mammalian retinal ganglion cells in culture. *Proceedings of the National Academy of Sciences of the U.S.A.* (in the Press).
- MARTY, A. (1981). Ca-dependent K channels with large unitary conductances in chromaffin cell membranes. *Nature* **291**, 497–500.
- MARTY, A. & NEHER, E. (1985). Potassium channels in cultured bovine adrenal chromaffin cells. *Journal of Physiology* **367**, 117–141.
- MARUYAMA, Y., GALLACHER, P. V. & PETERSEN, O. H. (1983). Cholecystokinin activation of single-channel currents is mediated by internal messenger in pancreatic acinar cells. *Nature* **302**, 827–829.
- MASLAND, R. H. & AMES III, A. (1976). Responses to acetylcholine of ganglion cells in an isolated mammalian retina. *Journal of Neurophysiology* **39**, 1220–1235.

- MEECH, R. W. (1978). Calcium-dependent potassium activation in nervous tissue. *Annual Review of Biophysics and Bioengineering* **7**, 1-18.
- MEECH, R. W. & STANDEN, N. B. (1975). Potassium activation in *Helix aspersa* neurones under voltage clamp: a component mediated by calcium influx. *Journal of Physiology* **249**, 211-239.
- MILLER, C., MOCZYDLOWSKI, E., LATORRE, R. & PHILLIPS, M. (1985). Charybdotoxin, a protein inhibitor of single  $\text{Ca}^{2+}$ -activated  $\text{K}^+$  channels from mammalian skeletal muscle. *Nature* **313**, 316-318.
- NEHER, E. & STEVENS, C. F. (1977). Conductance fluctuations and ionic pores in membranes. *Annual Review of Biophysics and Bioengineering* **6**, 345-381.
- NELSON, R., FAMIGLIETTI, E. V. & KOLB, H. (1978). Intracellular staining reveals different levels of stratification for on- and off-center ganglion cells in cat retina. *Journal of Neurophysiology* **41**, 472-483.
- NOWYCKY, M. C., FOX, A. P. & TSIEN, R. W. (1985). Three types of neuronal calcium channel with different agonist sensitivity. *Nature* **316**, 440-443.
- PALLOTA, B. S., MAGLEBY, K. L. & BARRETT, J. N. (1981). Single channel recordings of  $\text{Ca}^{2+}$ -activated  $\text{K}^+$  currents in rat muscle cell culture. *Nature* **293**, 471-474.
- PENNEFATHER, P., LANCASTER, B., ADAMS, P. R. & NICOLL, R. A. (1985). Two distinct Ca-dependent K currents in bullfrog sympathetic ganglion cells. *Proceedings of the National Academy of Sciences of the U.S.A.* **82**, 3040-3044.
- PERRY, V. H. (1979). The ganglion cell layer of the retina of the rat: a golgi study. *Proceedings of the Royal Society B* **204**, 363-375.
- SAITO, H.-A. (1981). The effects of strychnine and bicuculline on the responses of X- and Y-cells of the isolated eye-cup preparation of the cat. *Brain Research* **212**, 243-248.
- SAITO, H.-A. (1983). Morphology of physiologically identified X-, Y-, and W-type retinal ganglion cells of the cat. *Journal of Comparative Neurology* **221**, 279-288.
- SARTHY, P. V. & LAM, D. M. K. (1979). Isolated cells from a mammalian retina. *Brain Research* **176**, 208-212.
- SIGWORTH, F. J. (1980). The variance of sodium current fluctuations at the node of Ranvier. *Journal of Physiology* **307**, 97-129.
- STONE, J. & FUKADA, Y. (1974). Properties of cat retinal ganglion cells: a comparison of W-cells with X- and Y-cells. *Journal of Neurophysiology* **37**, 722-748.
- TACHIBANA, M. (1981). Membrane properties of solitary horizontal cells isolated from goldfish retina. *Journal of Physiology* **321**, 141-161.
- THOMPSON, S. H. (1977). Three pharmacologically distinct potassium channels in molluscan neurones. *Journal of Physiology* **265**, 465-488.
- WÄSSLE, H. & BOYCOTT, B. B. (1974). The morphological types of ganglion cells of the domestic cat's retina. *Journal of Physiology* **240**, 397-419.
- WÄSSLE, H., BOYCOTT, B. B. & ILLING, R. B. (1981). Morphology and mosaic of on- and off-beta cells in the cat retina and some functional considerations. *Proceedings of the Royal Society B* **212**, 177-195.
- WIESEL, T. N. (1959). Recording inhibition and excitation in the cat's retinal ganglion cells with intracellular electrodes. *Nature* **183**, 264-265.
- YELLEN, G. (1982). Single- $\text{Ca}^{2+}$ -activated nonselective cation channels in neuroblastoma. *Nature* **296**, 357-359.
- YPEY, D. L. & CLAPHAM, D. E. (1984). Development of a delayed outward-rectifying  $\text{K}^+$  conductance in cultured mouse peritoneal macrophages. *Proceedings of the National Academy of Sciences of the U.S.A.* **81**, 3083-3087.
- ZRENNER, E., NELSON, R. & MARIANI, A. (1983). Intracellular recordings from a biplexiform ganglion cell in Macaque retina, stained with horseradish peroxidase. *Brain Research* **1983**, 181-185.